



# Pressure-dependent calibration of the OH and HO<sub>2</sub> channels of a FAGE HO<sub>x</sub> instrument using the Highly Instrumented Reactor for Atmospheric Chemistry (HIRAC)

F. A. F. Winiberg<sup>1</sup>, S. C. Smith<sup>1</sup>, I. Bejan<sup>1</sup>, C. A. Brumby<sup>1</sup>, T. Ingham<sup>1,2</sup>, T. L. Malkin<sup>1,\*</sup>, S. C. Orr<sup>1</sup>, D. E. Heard<sup>1,2</sup>, and P. W. Seakins<sup>1,2</sup>

<sup>1</sup>School of Chemistry, University of Leeds, LS2 9JT, Leeds, UK

<sup>2</sup>National Centre for Atmospheric Science, University of Leeds, Leeds, LS2 9JT, UK

\* now at: Institute for Climate and Atmospheric Science, School of Earth and Environment, University of Leeds, Woodhouse Lane, Leeds, LS2 9JT, UK

Correspondence to: P. W. Seakins (p.w.seakins@leeds.ac.uk)

Received: 19 June 2014 – Published in Atmos. Meas. Tech. Discuss.: 31 July 2014

Revised: 25 November 2014 – Accepted: 20 December 2014 – Published: 3 February 2015

**Abstract.** The calibration of field instruments used to measure concentrations of OH and HO<sub>2</sub> worldwide has traditionally relied on a single method utilising the photolysis of water vapour in air in a flow tube at atmospheric pressure. Here the calibration of two FAGE (fluorescence assay by gaseous expansion) apparatuses designed for HO<sub>x</sub> (OH and HO<sub>2</sub>) measurements have been investigated as a function of external pressure using two different laser systems. The conventional method of generating known concentrations of HO<sub>x</sub> from H<sub>2</sub>O vapour photolysis in a turbulent flow tube impinging just outside the FAGE sample inlet has been used to study instrument sensitivity as a function of internal fluorescence cell pressure (1.8–3.8 mbar). An increase in the calibration constants  $C_{\text{OH}}$  and  $C_{\text{HO}_2}$  with pressure was observed, and an empirical linear regression of the data was used to describe the trends, with  $\Delta C_{\text{OH}} = (17 \pm 11)\%$  and  $\Delta C_{\text{HO}_2} = (31.6 \pm 4.4)\%$  increase per millibar air (uncertainties quoted to  $2\sigma$ ). Presented here are the first direct measurements of the FAGE calibration constants as a function of external pressure (440–1000 mbar) in a controlled environment using the University of Leeds HIRAC chamber (Highly Instrumented Reactor for Atmospheric Chemistry). Two methods were used: the temporal decay of hydrocarbons for calibration of OH, and the kinetics of the second-order recombination of HO<sub>2</sub> for HO<sub>2</sub> calibrations. Over comparable conditions for the FAGE cell, the two alternative methods are in good agree-

ment with the conventional method, with the average ratio of calibration factors (conventional: alternative) across the entire pressure range,  $C_{\text{OH}(\text{conv})}/C_{\text{OH}(\text{alt})} = 1.19 \pm 0.26$  and  $C_{\text{HO}_2(\text{conv})}/C_{\text{HO}_2(\text{alt})} = 0.96 \pm 0.18$  ( $2\sigma$ ). These alternative calibration methods currently have comparable systematic uncertainties to the conventional method:  $\sim 28\%$  and  $\sim 41\%$  for the alternative OH and HO<sub>2</sub> calibration methods respectively compared to 35% for the H<sub>2</sub>O vapour photolysis method; ways in which these can be reduced in the future are discussed. The good agreement between the very different methods of calibration leads to increased confidence in HO<sub>x</sub> field measurements and particularly in aircraft-based HO<sub>x</sub> measurements, where there are substantial variations in external pressure, and assumptions are made regarding loss rates on inlets as a function of pressure.

## 1 Introduction

Short-lived free radicals play a crucial role in determining the composition of the atmosphere. The catalytic cycle of HO<sub>x</sub> (= OH + HO<sub>2</sub>) radicals is of central importance to tropospheric chemistry. OH acts as the primary daytime oxidant, initiating the degradation of most trace gases and thereby controlling their atmospheric concentrations and lifetimes. The short lifetime of the radicals generate HO<sub>x</sub> concentrations which are uninfluenced by transport; therefore repro-

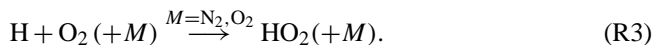
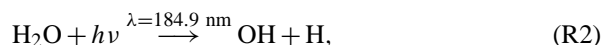
ducing observed HO<sub>x</sub> concentrations can be an excellent test of any chemical model (Heard and Pilling, 2003). However, it should be mentioned that agreement between measured and modelled [HO<sub>x</sub>] could be fortuitous as both sources and sinks of HO<sub>x</sub> radicals could be simultaneously under- or overestimated. The development of detection techniques that permit the speciation of a wider range of atmospheric components (e.g. volatile organic compounds (VOCs) and aerosols), together with OH reactivity measurements, can help to further constrain modelling studies and reduce the potential for the coincidental agreement. OH has been detected by long-path differential absorption spectroscopy (DOAS) in the field (Brauers et al., 1996; Dorn et al., 1996) and in the SAPHIR chamber (Schlosser et al., 2009), and chemical ionisation mass spectrometric techniques (CIMSs) have also been used in field observations (Eisele and Tanner, 1991; Berresheim et al., 2002; Sjostedt et al., 2007; Kukui et al., 2008). However, a majority of field measurements have been made using laser-induced fluorescence (LIF) spectroscopy, and intercomparisons exist which have validated the technique against DOAS and CIMS in both chamber (Schlosser et al., 2007, 2009; Fuchs et al., 2012) and field environments, including aircraft-based measurements (Eisele et al., 2001, 2003). Low concentrations and potential interferences (Fuchs et al., 2011; Mao et al., 2012; Whalley et al., 2013) make HO<sub>x</sub> measurements challenging. In addition, most HO<sub>x</sub> detection methods are not absolute, and hence calibration is required.

Fluorescence assay by gas expansion, FAGE, is a low-pressure LIF technique commonly used for the detection of OH and HO<sub>2</sub> radicals (Heard, 2006, and references therein). The low concentrations of ambient OH ( $\sim 10^6$  molecule cm<sup>-3</sup>) require a viable measurement technique to discriminate between laser-scattered light and small signal levels. Originally this was attempted by exciting OH to the first vibrational level in the A state at 282 nm ( $A^2\Sigma^+$  ( $\nu' = 1$ )  $\leftarrow X^2\Pi_i$  ( $\nu'' = 0$ )) OH transition) and observing off-resonant fluorescence at  $\sim 308$  nm using an interference filter to help discriminate against scattered laser radiation (Davis et al., 1976). Although non-resonant LIF has been successful in stratospheric applications (Wennberg et al., 1994), in the troposphere 282 nm photolysis of ozone (and subsequent reaction of O(<sup>1</sup>D) with water vapour) generates an unacceptably high interfering OH signal, and on-resonant LIF with excitation at 308 nm is used instead. Expanding the sample through a pinhole to low pressure ( $\sim 1$ – $2$  Torr) increases the fluorescence lifetime of the A state beyond the laser scatter pulse, allowing for temporal discrimination against the resonant 308 nm excitation pulse ( $A^2\Sigma^+$  ( $\nu' = 0$ )  $\leftarrow X^2\Pi_i$  ( $\nu'' = 0$ )) OH transition). Injection of an OH scavenger (e.g. C<sub>3</sub>F<sub>6</sub>) allows quantification of any laser-generated OH interference (Mao et al., 2012; Novelli et al., 2014). HO<sub>2</sub> is converted into OH via reaction with added NO:



and the resultant OH is detected in the same way. Detection of OH and HO<sub>2</sub> either simultaneously or in series can be achieved using the same LIF detection axis (measurements in series; Creasey et al., 1997a), with two separate LIF axes within the same cell (simultaneous; Stevens et al., 1994) or with two separate detection cells (simultaneous; Whalley et al., 2010).

LIF is a very sensitive but non-absolute detection method, and therefore each channel of the instrument needs to be calibrated. The vacuum-ultraviolet (VUV) photolysis of H<sub>2</sub>O vapour was originally developed for the calibration of HO<sub>x</sub> measurement instruments in the 1990s (Aschmutat et al., 1994; Schultz et al., 1995; Heard and Pilling, 2003). Since then the methodology has become the HO<sub>x</sub> measurement community standard. Upon the photolysis of a known H<sub>2</sub>O vapour concentration (in synthetic air at atmospheric pressure) by a mercury (Hg) Pen-Ray lamp at 184.9 nm, OH and HO<sub>2</sub> are produced in unity ratio (Fuchs et al., 2011) via Reactions (R2) and (R3) (Schultz et al., 1995):



The radicals are then sampled by the HO<sub>x</sub> instrument at atmospheric pressure; the concentrations of OH and HO<sub>2</sub> produced can be determined using Eq. (1):

$$[\text{OH}] = [\text{HO}_2] = [\text{H}_2\text{O}] \sigma_{\text{H}_2\text{O}, 184.9 \text{ nm}} \Phi_{\text{OH}} F_{184.9 \text{ nm}} \Delta t, \quad (1)$$

where [H<sub>2</sub>O] is the water vapour concentration;  $\sigma_{\text{H}_2\text{O}, 184.9 \text{ nm}}$  is the known absorption cross section of H<sub>2</sub>O vapour at 184.9 nm ( $(7.22 \pm 0.22) \times 10^{-20}$  cm<sup>2</sup> molecule<sup>-1</sup> (Cantrell et al., 1997; Creasey et al., 2000));  $\Phi_{\text{OH}}$  ( $= \Phi_{\text{HO}_2} = 1$ ) is the photodissociation quantum yield of OH and HO<sub>2</sub> (Fuchs et al., 2011);  $F_{184.9 \text{ nm}}$  is the photon flux of 184.9 nm light; and  $\Delta t$  is the exposure time of the air to the Hg lamp output. There are two main methodologies used for obtaining the product  $F_{184.9 \text{ nm}} \Delta t$  in Eq. (1). In the first, the two parameters are measured separately,  $F_{184.9 \text{ nm}}$  using a calibrated phototube and  $\Delta t$  using knowledge of the volumetric flow rate and geometric parameters of the flow tube (Stevens et al., 1994). In the other, a chemical actinometer is used to obtain the product directly, with both O<sub>2</sub> and N<sub>2</sub>O photolysis at 184.9 nm used to generate either O<sub>3</sub> or NO, which is subsequently detected using commercial analysers, with good sensitivity (Creasey et al., 1997a; Hofzumahaus et al., 1997; Heard and Pilling, 2003; Faloon et al., 2004). There are two main methods for delivery of the OH radicals to the FAGE inlet at atmospheric pressure, either using a laminar or turbulent flow tube. In the laminar flow regime there is a radial gradient in the OH concentration for which the so-called profile factor ( $P$ ) has to be quantified (Holland et al., 1995; Creasey et al., 1997a), whereas in a turbulent flow system the radial OH concentration is constant except very close to the walls.

Alternative calibration methods have also been developed, but typically not deployed in the field, and examples of these will be employed in the current study. A detailed evaluation of calibration techniques has been presented by Dusanter et al. (2008). In some of the earliest field measurements, Hard et al. (1995) developed a calibration method based on hydrocarbon decays. The concentration of a hydrocarbon with a known and well-characterised rate coefficient for reaction with OH,  $k$  (in this case 1,3,5-trimethylbenzene), was measured as a function of time using gas chromatography, allowing determination of all the parameters in Eq. (2) with the exception of [OH]. The rate of loss of a hydrocarbon (HC) through reaction with OH is given by Eq. (2):

$$\frac{d[\text{HC}]}{dt} = k [\text{OH}][\text{HC}]. \quad (2)$$

This methodology has also been applied more recently to FAGE validation measurements in the EUPHORE chamber (Bloss et al., 2004).

For HO<sub>2</sub> the well-defined second-order recombination rate coefficient for Reaction (R4) can be used to determine [HO<sub>2</sub>], where for a second-order reaction the half-life of the decay is related to the initial starting concentration.



In a short set of experiments, Pilling et al. (2005) generated HO<sub>2</sub> from the photolysis of formaldehyde in the EUPHORE chamber and observed the second-order HO<sub>2</sub> decay with a FAGE instrument. The decays were in good agreement with the calibrated HO<sub>2</sub> measurements, but no systematic studies have been undertaken using this reaction as a calibration method.

The deployment of the FAGE technique for aircraft-based measurements (Faloona et al., 2000; Commane et al., 2010; Martinez et al., 2010) raises two issues. First, the need to sample air from outside of the boundary layer of the aircraft fuselage requires a significant length of flow tube before the gas sample is interrogated by the laser beam. Secondly, the pressure in the FAGE cell will vary as the aircraft changes altitude (e.g. 0–7 km, 1.3–2.8 mbar internal cell pressure range, from Commane et al., 2010), altering the instrumental sensitivity (Commane et al., 2010; Martinez et al., 2010) owing to changes, for example, in the nature of the initial expansion into the FAGE apparatus. The current design of the flow tube calibration method is limited to delivering the calibrated [OH] at atmospheric pressure; however, by using different nozzle pinhole diameters (typically 0.2–1.0 mm) it is possible to alter the pressure in the FAGE cell over the range typically encountered during a flight. Importantly, this method does not compensate for the changing pressure differential across the inlet nozzle experienced during a flight and what effect this might have on the expanding gas before it reaches the FAGE cell. The possible changes in radical surface losses due to the change in inlet pinhole diameter are also assumed to be negligible.

Potential systematic uncertainties around the application of calibrations performed at atmospheric pressure to HO<sub>x</sub> data obtained whilst sampling from different pressures (e.g. in flight) highlight the need to obtain calibrations at relevant external pressures. Martinez et al. (2010) have investigated the effect of external pressure on instrument sensitivity by calibrating during flight, reporting an increase in the instrument sensitivity to OH in the free troposphere, compared to the boundary layer. It was not concluded whether this was an effect of the calibration source used (conventional H<sub>2</sub>O vapour photolysis) or the instrument itself; however the increase was not characterised by the conventional calibrations performed on the ground before the flight.

We report here an intercomparison of HO<sub>x</sub> calibrations based on the conventional flow tube methodology, using different inlet nozzle diameters to vary the internal fluorescence cell pressure, with two alternative calibration methods. Analysis of the decays of hydrocarbons was used to determine [OH], while analysis of the kinetics of HO<sub>2</sub> decay by self-reaction following the photolysis of formaldehyde was used to determine [HO<sub>2</sub>]. The studies took place in the Highly Instrumented Reactor for Atmospheric Chemistry (HIRAC), which is a custom-built atmospheric simulation chamber providing the unique ability to simultaneously vary pressure and temperature whilst measuring the short-lived free radical species OH, HO<sub>2</sub> and NO<sub>3</sub> (Glowacki et al., 2007a; Malkin, 2010; Malkin et al., 2010). These features make HIRAC ideally suited to the study of the kinetics and mechanisms of atmospherically relevant reactions and the calibration, validation and development of atmospheric measurement instrumentation.

## 2 HIRAC and FAGE instrumentation

### 2.1 HIRAC

Experiments were conducted in HIRAC, a stainless-steel chamber with a total volume of 2.25 m<sup>3</sup> and total internal surfaces of 13 m<sup>2</sup> ( $S/V \sim 5.8 \text{ m}^{-1}$ ). The chamber could operate over a wide range of pressures (10–1000 mbar), with multiple access ports used to connect an array of instrumentation and monitoring equipment (pressure gauges, thermocouples etc.). Further details on the construction can be found in Glowacki et al. (2007a) and Malkin et al. (2010).

The photolysis lamps, housed in eight quartz tubes mounted radially inside the reactive volume, were used to initiate photochemistry. The lamps were interchangeable depending on the target molecules; lamps, with primary emissions centred at 254 and 290 nm (GE Optica, GE55T8/HO and Philips, TL40W/12 RS), were used for the alternative OH and HO<sub>2</sub> calibration methods respectively (Sects. 3.2 and 3.3). The output of the lamps was temperature dependent outside of a narrow temperature range ( $\sim 35\text{--}39^\circ\text{C}$ ), and so the housings were flushed with N<sub>2</sub> to regulate the temperature

and remove photolabile species. A photolysis-lamp-induced chamber temperature increase of  $\sim 2$  K was seen over the course of a typical experiment ( $< 40$  min), and was therefore considered negligible compared to the temperature of the chamber on any given day ( $293 \pm 5$  K).

Investigations into radical gradients across the HIRAC chamber have been conducted using direct FAGE measurements of OH produced from both photolytic (methyl nitrite) and non-photolytic ( $\text{O}_3 + \text{trans-2-butene}$ ) sources using an extended inlet (800 mm) to probe across the chamber diameter. No significant OH radical gradient was observed until the FAGE sampling nozzle was  $\sim 200$  mm from the wall and a maximum  $\sim 15\%$  decrease (compared to the centre of the chamber) was seen when the sampling inlet was flush with the chamber walls. Other than being close to the walls, the lack of gradient in OH radicals from both photolytic and non-photolytic sources provides direct evidence of the homogeneity of the lamp radiation profile and efficacy of mixing in the chamber, whilst showing that the standard FAGE inlet (280 mm, Sect. 2.2) samples well into the homogeneous area.

Ozone was monitored using a UV photometric  $\text{O}_3$  analyser (Thermo Electron Corporation 49C, detection limit (d.l.) = 1.0 ppbv at 60 s averaging). The  $\text{O}_3$  analyser had been calibrated using a commercial ozone primary standard (Thermo Electron Corporation 49i-PS), and an intercomparison with the Fourier transform infrared (FTIR) spectroscopy within HIRAC was linear (Glowacki et al., 2007a). A chemiluminescence  $\text{NO}_x$  analyser (TEC 42C, d.l. = 50 pptv at 60 s averaging) was used to determine that levels of  $\text{NO}_x$  ( $= \text{NO} + \text{NO}_2$ ) were characteristically below the detection limit of the apparatus.

A calibrated gas chromatography instrument with flame ionisation detector (GC-FID, Agilent Technologies, 6890N) was used for the online detection of reactants (Sect. 3.2) using an evacuated sampling loop into which gas from the chamber was expanded. The GC was fitted with a CP-SIL-5 column (50 m, 0.32 mm, 5  $\mu\text{m}$ ) using He carrier gas and a constant oven temperature (40–75  $^\circ\text{C}$  depending on the hydrocarbon being detected) and was able to provide hydrocarbon measurements on a 2–6 min time resolution. Supporting measurements of *iso*-butene and  $(\text{CH}_3)_3\text{COOH}$  were made via a long-path FTIR absorption facility. The FTIR spectrometer (Bruker, IFS/66) was coupled to a Chernin-type multipass cell (Glowacki et al., 2007b) and spectral resolution was maintained at  $1 \text{ cm}^{-1}$  across all experiments, using 32 co-added spectra for a 30 s time resolution.

Calibration experiments were conducted over a pressure range of 440–1000 mbar in an ultra-high-purity (UHP) 1 : 4 synthetic air mix of  $\text{O}_2$  (BOC, zero-grade,  $> 99.999\%$ ) and  $\text{N}_2$  (BOC, zero-grade,  $> 99.998\%$ ) to match the range of pressures from the pinhole calibration method (Sect. 3.1). The UHP gases help maintain low  $\text{H}_2\text{O}$  vapour ( $< 10$  ppm, verified by dew-point hygrometer measurement),  $\text{NO}_x$  ( $< 1$  ppbv) and non-methane hydrocarbons ( $< 1$  ppbv) during experimental runs. Thorough mixing of reaction mix-

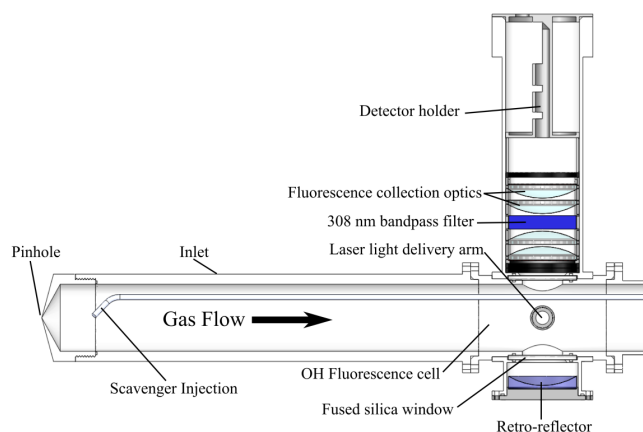


**Figure 1.** Schematic showing a side-on vertical cross section of the HIRAC FAGE OH fluorescence cell. The OH scavenger (*iso*-butane) was introduced  $\sim 40$  mm from the inlet pinhole through an  $1/8$  in. internal-diameter stainless-steel tube mounted in between the OH and  $\text{HO}_2$  cells (out of frame). The tube ran flush to the cell wall to reduce possible scattering of laser light, and the tip was angled slightly towards the centre of the main gas flow to improve mixing.

tures within HIRAC was achieved in  $\leq 70$  s by four vibrationally damped, variable speed circulation fans mounted in pairs at each end of the chamber. The chamber was evacuated to  $\sim 0.05$  mbar for  $\sim 60$  min following each experiment using a rotary-pump-backed roots blower (Leybold, trivac D40B and ruvac WAU251) to ensure removal of all reactants/products. Known concentrations of precursors were introduced to the chamber in the vapour phase through a 0.97 L stainless-steel delivery vessel. A combined sampling rate of  $\sim 9$  sLm from the chamber required a counter flow of synthetic air maintaining the desired pressure and diluting the reactants ( $(4.5 \pm 0.2) \times 10^{-5} \text{ s}^{-1}$ ). This was regulated using two Brooks mass flow controllers ( $\text{N}_2$  and  $\text{O}_2$ ).

## 2.2 $\text{HO}_x$ detection instrument

Calibrations were conducted using both the University of Leeds aircraft- and HIRAC-based FAGE instruments, brief operational details of which are shown in Table 1. The two FAGE systems were very similar in design except for the inlet length and pinhole size as highlighted in Table 1. The aircraft instrument was used as described in Commane et al. (2010) to validate the alternative  $\text{HO}_2$  calibration technique only. The HIRAC-based FAGE instrument has also been described in the literature by Glowacki et al. (2007a), and hence only modifications since publication will be discussed here.

Figure 1 shows the cross-sectional schematic of the HIRAC FAGE instrument. Under typical operating conditions, air was sampled at  $\sim 6$  sLm through a 1.0 mm diameter pinhole nozzle and passed down the inlet (length 280 mm,

**Table 1.** FAGE instruments used and their respective inlet designs, laser systems and calibration methods used.

FAGE instrument	Inlet design	Pinhole diameter	Length	Laser	Calibrations conducted
Aircraft	Pinhole diameter	0.6 mm	420 mm	Photonics Industries (5 kHz PRF) Nd:YAG (DS-532-10) pumped Ti:Sa (TU-UV-308)	H <sub>2</sub> O vapour photolysis, HCHO photolysis
	Length				
HIRAC	Pinhole diameter	1.0 mm	280 mm	Litron, NANO-TRL-250, (200 Hz PRF) Nd:YAG pumped dye laser (Lambda Physik, LPD3000)	H <sub>2</sub> O vapour photolysis, HCHO photolysis, HC decay
	Length				

50 mm diameter) into the OH detection axis maintained at low pressure (1.8–3.85 mbar) using a high capacity rotary-backed roots blower pumping system (Leybold, trivac D40B and ruvac WAU251). Using the same pump set, the aircraft instrument was operated with a 420 mm long inlet and a 0.6 mm pinhole. The long inlet was used to draw a sample away from the chamber walls where radical losses become significant (see Sect. 2.1). Both instruments were coupled to the HIRAC chamber using custom-made ISO-K160 flanges, ensuring the pinhole, in both cases, was kept  $\sim 225$  mm from the chamber walls.

Concentrations of HO<sub>2</sub> were measured simultaneously in a second detection axis  $\sim 300$  mm downstream of the OH detection axis. High-purity NO (BOC, N2.5 nitric oxide) was added  $\sim 20$  mm before the HO<sub>2</sub> detection axis into the centre of the FAGE cell in the direction of gas flow through 1/8 in. stainless-steel tubing at a rate of 5 sccm (Brooks 5850S), converting HO<sub>2</sub> to OH.

Recently published material on the conversion of certain RO<sub>2</sub> radicals to OH upon reaction with NO in FAGE detection cells (Fuchs et al., 2011; Whalley et al., 2013) has shown a significant enhancement of the HO<sub>2</sub> signal in the presence of RO<sub>2</sub> derived from certain hydrocarbons. These effects have been thoroughly studied using a range of different hydrocarbons for the HIRAC FAGE apparatus and will be the subject of a further publication. The potential interferences associated with HO<sub>2</sub> measurements in the presence of certain hydrocarbons due to the presence of  $\beta$ -hydroxyperoxy radicals do not apply to either HO<sub>2</sub> calibration method. In addition, any interference from RO<sub>2</sub> radicals produced during the alternative calibration methods was experimentally demonstrated to be negligible under the conditions of these experiments (Winiberg, 2014).

Experiments with the HIRAC FAGE instrument used a new medium pulse repetition frequency (PRF) laser light source (= 200 Hz), with a different light delivery method to the detection cells, compared to that described by Glowacki et al. (2007a). The previously used JDSU Nd:YAG pumped Sirah Cobra Stretch system (PRF = 5 kHz) focussed the frequency-doubled 308 nm output into fibre optic cables

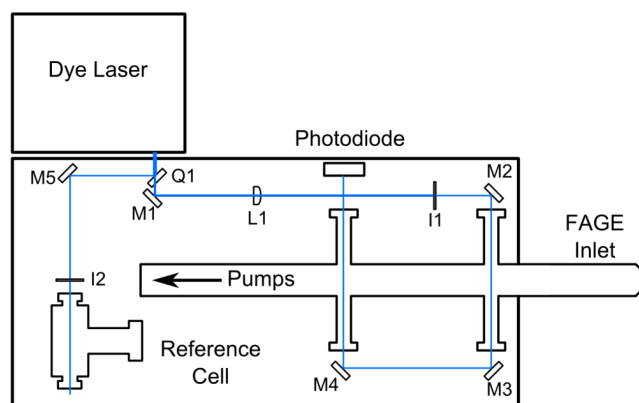


**Figure 2.** Top-down schematic of the FAGE instrument showing the laser beam path (blue line) through the OH and HO<sub>2</sub> detection cells, and the reference cell using the Litron/LPD3000, 200 Hz PRF laser source. Q – quartz flat; M – mirror; I – iris; and L – lens. The FAGE inlet is extended past the edge of the mounting table for insertion into the HIRAC chamber. The calibrated photodiode was used to normalise the fluorescence signals to fluctuations in laser power.

(10 m, Oz Optics), which were then attached directly to the FAGE cell arms via collimators (Oz Optics). Using the new Litron Nd:YAG (NANO-TRL-50-250) pumped Lambda Physik (LPD3000) dye laser system (PRF = 200 Hz), the high laser pulse energies were found to burn the ends of the fibre optic cables, and hence direct light delivery was applied using a combination of mirrors, lenses and irises to direct and shape the beam to the OH and HO<sub>2</sub> detection regions, as shown in the top-down schematic of the modified HIRAC FAGE instrument displayed in Fig. 2.

The UV light exiting the dye laser was split with a quartz flat (Fig. 2, Q1) to direct  $\sim 5\%$  of the laser light towards the reference cell (where OH was generated continuously from a hot wire filament in water-saturated air), which enabled precise tuning of the laser wavelength to the maxima of the OH Q1 (2) branch (within 98%). The remaining light was aligned through the OH and HO<sub>2</sub> cells sequentially using a series of 308 nm centred turning optics (M1–M4, CVI Laser

Optics, Melles Griot). A lens was used ( $L1$ ,  $f = 100$  mm) in conjunction with an iris ( $I2$ ), to help transmit the laser beam through both detection cells, avoiding collisions with any internal surfaces. Fluctuations in laser power were accounted for using a linear-response, UV-sensitive photodiode (UDT-555UV, Laser Components UK) at the exit arm of the  $\text{HO}_2$  detection axis to normalise the LIF signal. Both laser systems provided 5–7 and 2–3 mW of 308 nm light to the OH and  $\text{HO}_2$  detection axes respectively.

The OH fluorescence was collected orthogonal to the gas flow onto electronically gated Channeltron PhotoMultiplier tubes (CPM, Perkin Elmer, C943P) via a series of imaging lenses and a narrow-bandpass filter (Barr Associates,  $308.8 \pm 5.0$  nm). A spherical concave back reflector was positioned underneath the cell, opposite the detection optics, to optimise light collection onto the CPM. To avoid detector saturation, the CPM was gated (i.e. switched off) for the duration of the laser pulse using a modified gating unit based on the original design by Creasey et al. (1997a). Signals from the CPM were analysed using photon-counting cards (Becker and Hickl PMS-400A).

A new OH scavenger system was installed to help discriminate between OH sampled from the chamber and laser-generated OH in the fluorescence cells due to the higher pulse energies associated with the 200 Hz PRF laser system ( $1 \times 10^{14}$  compared to  $5 \times 10^{12}$  photons pulse $^{-1}$  cm $^{-2}$  at 5 kHz for laser power = 8 mW). A mixture of *iso*-butane (20% in  $\text{N}_2$ ) was injected  $\sim 40$  mm inside the inlet pin-hole into the central flow (Fig. 1), through a 1/8 in. internal-diameter stainless-steel pipe at a rate of  $\sim 20$  sccm, reacting with the sampled OH before reaching the detection axis. The laser-generated OH was probed within the same laser pulse (12 ns) and hence was not suppressed by the scavenger injection. Multiple photolysis of the same gas sample was avoided as the residence time in the laser pulse cross section ( $\sim 0.5$  cm $^2$ ) was calculated at  $\sim 0.4$  ms, compared to a laser pulse every 5 ms at 200 Hz PRF (assuming plug flow at a 6 sLm ambient sampling rate). Neither a pressure increase nor attenuation of UV light was detected during the scavenger injection process at this flow rate and dilution.

### 3 Calibration procedures

#### 3.1 Conventional $\text{H}_2\text{O}$ vapour photolysis calibration

The requisite equation for calibration of FAGE by water vapour photolysis was given as

$$[\text{OH}] = [\text{HO}_2] = [\text{H}_2\text{O}] \sigma_{\text{H}_2\text{O}, 184.9\text{nm}} \Phi_{\text{OH}} F_{184.9\text{nm}} \Delta t \quad (3)$$

and the principles were outlined above in Sect. 1. A schematic diagram of the  $\text{H}_2\text{O}$  vapour photolysis calibration source is presented in Fig. 3, consisting of a square cross-section flow tube ( $12.7 \times 12.7 \times 300$  mm) through which 40 sLm of humidified air (BOC, BTCA 178) was

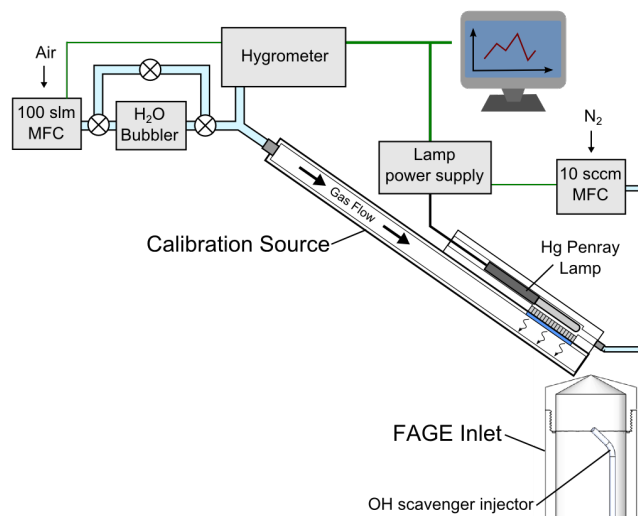


**Figure 3.** Schematic cross section of the  $\text{H}_2\text{O}$  vapour photolysis calibration source used in the calibration of the two FAGE instruments (inlet for HIRAC FAGE instrument shown here, for example). The  $[\text{H}_2\text{O}]_{\text{vapour}}$  was measured prior to entering the square cross-section flow tube, and the concentration was controlled through a series of three taps around the bubbler. The Hg Pen-Ray lamp was housed in a second section of the wand, and the output was collimated through a Suprasil window using a honeycomb arrangement of  $\phi = 1$  mm aluminium tubes. The lamp was continuously flushed with  $\text{N}_2$  to remove potential absorbers and photolabile species, and to help regulate temperature.

passed, resulting in a turbulent flow regime (Reynolds number  $\geq 4000$ ). The air was humidified by passing a fraction of the total air flow through a deionised water bubbler system, and  $[\text{H}_2\text{O}]$  was measured using a dew-point hygrometer (CR4, Buck Research Instrument) prior to the flow tube. The collimated 184.9 nm output of a mercury Pen-Ray lamp (LOT-Oriel, Hg-Ar) was introduced to the end of the main flow tube, photolysing  $\text{H}_2\text{O}$  vapour (Reactions R2–R3). The gas output from the flow tube was directed towards the FAGE sampling inlet, where the overflow of the FAGE sample volume from the flow tube stopped the impingement of ambient air. A range of  $\text{HO}_x$  concentrations were produced by changing both the  $\text{H}_2\text{O}$  vapour concentration and the mercury lamp photon flux.

The flux of 184.9 nm light,  $F_{184.9\text{nm}}$ , was varied by altering the Hg lamp supply current and was dependent on the specific mercury lamp employed along with the lamp temperature and orientation (Hofzumahaus et al., 1997; Creasey et al., 2000; Dusanter et al., 2008). To this end, determinations of the flux from the specific mercury lamp used in the calibrations described in this work were made in situ for lamp supply currents between 0.2 and 3.0 mA using the  $\text{N}_2\text{O}$  actinometry method described in detail in a number of publications (Edwards et al., 2003; Heard and Pilling, 2003; Faloon et al., 2004; Glowacki et al., 2007a; Whalley et al., 2007).

The exposure time of the air to the 184.9 nm light,  $\Delta t$ , was calculated as a function of the known velocity of the air and the cross section of the photolysis region.

Various cell conditions and their effect on the sensitivity to OH and HO<sub>2</sub> have been reported in the literature (Faloona et al., 2004; Martinez et al., 2010; Regelin et al., 2013). Here, instrument sensitivity as a function of internal cell pressure has been determined for the HIRAC FAGE instrument using the 200 Hz PRF laser source only (Table 1). Different internal cell pressures (1.8–3.8 mbar) were achieved by changing the diameter of the FAGE inlet pinhole between 0.5 and 1.0 mm. For the aircraft FAGE instrument, inlet pinhole diameters between 0.3 and 0.6 mm were used giving internal cell pressures between 1.4 and 2.5 mbar.

### 3.2 Hydrocarbon decay method – OH calibration

Hydrocarbons ( $0.5\text{--}2.0 \times 10^{13}$  molecule cm<sup>-3</sup>) and the OH precursor, *tert*-Butyl hydroperoxide (TBHP, Sigma Aldrich  $\sim 40\%$  in H<sub>2</sub>O,  $2.0 \times 10^{13}$  molecule cm<sup>-3</sup>) were introduced to the chamber before the lamps were switched on, initiating the decay experiment. OH was produced directly from the photolysis of TBHP at  $\lambda = 254$  nm and is, as far as we are aware, the first chamber experiment to use TBHP photolysis as a source of NO<sub>x</sub>-free OH. Upon illumination of the chamber, rapid photolysis led to an instantaneous peak [OH]  $\sim 10^7$  molecule cm<sup>-3</sup> before OH decayed away over  $\sim 30$  min as the TBHP was removed by photolysis, whilst OH was removed through reaction with TBHP ( $k_{\text{OH}}(296\text{ K}) = (3.58 \pm 0.54) \times 10^{-12}$  cm<sup>3</sup> molecule<sup>-1</sup> s<sup>-1</sup>; Baasandorj et al., 2010) and the selected hydrocarbon. The alternative OH calibrations presented here were conducted for the HIRAC-based FAGE instrument operating at 200 Hz PRF only.

Cyclohexane (> 99%, Fisher Scientific), *n*-pentane (> 99%, Fisher Scientific) and *iso*-butene (99%, Sigma Aldrich) were employed as the hydrocarbons in this study due to their sufficiently fast and well-known rates of reaction with OH to provide a quantifiable decay compared to chamber dilution. The rate coefficient for OH with *iso*-butene has been evaluated by IUPAC as  $k_{\text{OH}}(298\text{ K}) = (51 \pm 12) \times 10^{-12}$  cm<sup>3</sup> molecule<sup>-1</sup> s<sup>-1</sup> (IUPAC, 2007), and rate coefficients for the reaction of OH with cyclohexane and *n*-pentane have been reviewed by Calvert et al. (2008) as  $k_{\text{OH}}(298\text{ K}) = (6.97 \pm 1.39)$  and  $(3.96 \pm 0.76) \times 10^{-12}$  cm<sup>3</sup> molecule<sup>-1</sup> s<sup>-1</sup> respectively (all quoted to  $\pm 2\sigma$ ). Whilst alkanes are known to have a pressure-independent rate coefficient for OH reactions, the reactions of OH with alkenes occur predominantly by addition, a process which is pressure dependent, with the rate coefficient increasing with pressure up to the high-pressure limit where the addition of OH is the rate-determining step (Pilling and Seakins, 1995). A study by Atkinson and Pitts (1975) into the reaction of various small-chain alkenes showed no pressure dependence for

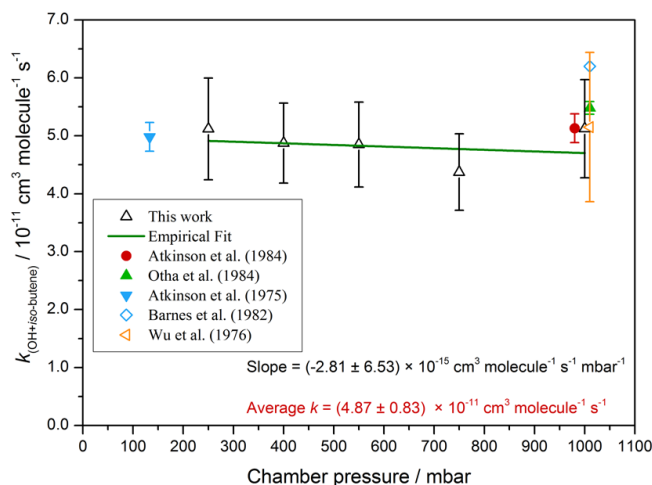


**Figure 4.** Rate constant,  $k_{\text{OH}}$ , for *iso*-butene + OH over the 250–1000 mbar pressure range measured relative to an isoprene reference in the HIRAC chamber. An empirical linear least-squares fit to the data is shown to emphasise lack of observed pressure dependence in the measured rate constant. Error bars represent the standard error ( $\pm 1\sigma$ ) in the associated relative rate determination of  $k_{\text{OH}}$ , and linear regression is weighted to account for this.

propene over 33–133 mbar of argon; therefore the reaction of OH with the larger *iso*-butene molecule is presumed to be pressure independent above 133 mbar (Atkinson, 1986; Atkinson et al., 2004). To confirm this, a relative rate study in air was conducted using isoprene as a reference ( $k_{\text{OH}}(298\text{ K}) = (1.00 \pm 0.14) \times 10^{-10}$  cm<sup>3</sup> molecule<sup>-1</sup> s<sup>-1</sup>, IUPAC, 2007). Both direct and relative rate studies have shown that the reaction of isoprene and OH is at the high-pressure limit above 100 Torr (Campuzano-Jost et al., 2004; Park et al., 2004; Singh and Li, 2007). Figure 4 shows that there is no significant pressure dependence in  $k_{\text{OH}}$  for OH + *iso*-butene over the 250–1000 mbar pressure range within the uncertainty of the experiment ( $\sim 25\%$ ,  $\pm 2\sigma$ ) and that the measured rate coefficient,  $k_{\text{OH}}(298\text{ K}) = (4.87 \pm 0.83) \times 10^{-11}$  cm<sup>3</sup> molecule<sup>-1</sup> s<sup>-1</sup>, is in good agreement with the literature values ( $(5.07 \pm 0.51) \times 10^{-11}$  cm<sup>3</sup> molecule<sup>-1</sup> s<sup>-1</sup> for IUPAC; Atkinson, 2003; IUPAC, 2007).

The hydrocarbon decay method relies on the loss of hydrocarbon being solely due to reaction with OH, and hence the effects of O<sub>3</sub> and NO<sub>3</sub> as reagents must be considered as both are important in the oxidation of alkenes (Atkinson, 1994). Before photolysis, O<sub>3</sub> and NO<sub>x</sub> were measured to be around the instrumental detection limits (0.5 and 0.050 ppb at 60 s averaging respectively) using commercial analysers (details given in Sect. 2.1). Upon photolysis a slow increase in O<sub>3</sub> and NO<sub>2</sub> was observed, to a maximum of  $\sim 40$  and  $\sim 20$  ppbv respectively. The [NO<sub>3</sub>] upper limit was estimated at  $\sim 0.32$  pptv using a simple steady-state approximation, where NO<sub>3</sub> production was controlled purely by

$\text{O}_3 + \text{NO}_2 \rightarrow \text{NO}_3$  (Atkinson et al., 2004) and loss by photolysis ( $j(\text{NO}_2) = 1.93 \pm 0.10$ ; Glowacki et al., 2007a). Under these conditions it was estimated that > 98 % of the loss of *iso*-butene would be due to OH and not  $\text{O}_3$  or  $\text{NO}_3$  where  $k_{\text{O}_3} = (1.13 \pm 0.33) \times 10^{-17} \text{ cm}^3 \text{ molecule}^{-1} \text{ s}^{-1}$  and  $k_{\text{NO}_3} = (3.4 \pm 1.0) \times 10^{-13} \text{ cm}^3 \text{ molecule}^{-1} \text{ s}^{-1}$  (Calvert et al., 2000).

### 3.3 Formaldehyde photolysis – $\text{HO}_2$ calibration

Formaldehyde was produced by direct heating of paraformaldehyde powder in a glass finger (Sigma Aldrich, 99 %) and was introduced in a flow of nitrogen into the chamber at concentrations  $\sim 2 \times 10^{13} \text{ molecule cm}^{-3}$  (determined manometrically). The chamber was irradiated (lamps: Philips TL40W/12 RS), resulting in an almost instantaneous  $\text{HO}_2$  signal. Once an approximately steady-state  $\text{HO}_2$  concentration was achieved, the photolysis lamps were turned off and the decay of  $\text{HO}_2$  was monitored by FAGE for  $\sim 120 \text{ s}$  until near-background signals levels were reached. The measurement of  $\text{HO}_2$  decays was repeated up to five times before the laser wavelength was scanned to the offline position. Therefore five individual  $C_{\text{HO}_2}$  determinations could be achieved from one chamber fill, with the limiting factor being the increased complexity of the reaction mixture after repeated photolysis cycles. After five decays, the analysis often exhibited evidence of secondary chemistry starting to distort the  $\text{HO}_2$  signal profiles, showing non-linearity in second-order plots. The absence of OH in these experiments was confirmed by simultaneous measurement of OH in the OH fluorescence cell, giving signals below the detection limit ( $1.6 \times 10^6 \text{ molecule cm}^{-3}$  for 60 s averaging for the 200 Hz PRF laser system).

Formaldehyde concentrations were kept low ( $< 3 \times 10^{13} \text{ molecule cm}^{-3}$ ) to avoid removal of  $\text{HO}_2$  via reaction with HCHO, ensuring that the loss of  $\text{HO}_2$  occurs predominately via self-reaction and wall loss (Sect. 4.2). The  $\text{HO}_2$  calibrations were conducted for the HIRAC-based FAGE instrument operating at 200 Hz PRF and the aircraft-based FAGE instrument operating at 5 kHz PRF. The chamber mixing fans were used for the majority of calibration data sets discussed here, representative of a typical experimental homogeneous gas mixture. A series of experiments were conducted without the mixing fans to probe the  $\text{HO}_2$  recombination and wall-loss kinetics using the aircraft-based FAGE instrument, and these are discussed in greater detail in Sects. 4.2 and 5.3.

## 4 Data analysis

### 4.1 Hydrocarbon decay

Figure 5 shows the hydrocarbon decay for *iso*-butene at 750 mbar and 294 K measured by GC-FID and FTIR. Using the Guggenheim method (Guggenheim, 1926; Bloss et

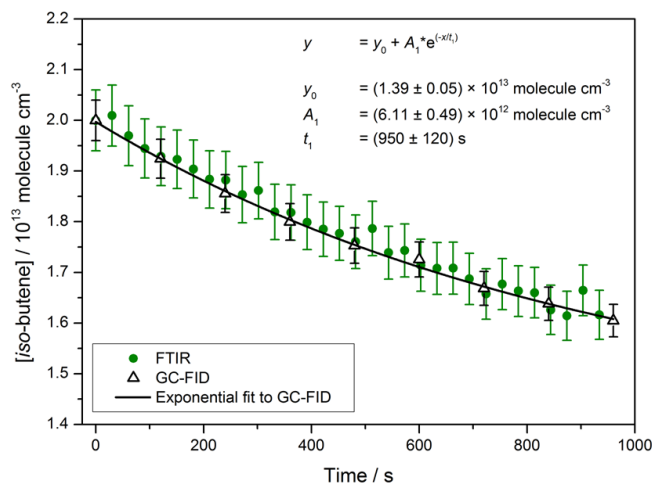


**Figure 5.** Decay of *iso*-butene as a function of time through reaction with OH in HIRAC (750 mbar, 294 K), measured using GC-FID on a 2 min time resolution. The data are fitted with a first-order exponential decay (purely empirical) to allow calculation of [HC] on the same timescale as the 60 s averaged FAGE data. Time = 0 s indicates photolysis lamp turn-on time and uncertainties are quoted to  $\pm 1\sigma$ . Error bars are representative of the precision in the GC-FID ( $\sim 2\%$ ) and FTIR ( $\sim 3\%$ ) measurements to  $1\sigma$ .

al., 2004) the pseudo-first-order rate coefficient ( $k'$ ) for the hydrocarbon removal was calculated using Eq. (3):

$$k' = \frac{\ln([\text{HC}]_1/[\text{HC}]_2)}{(t_2 - t_1)}, \quad (4)$$

where  $[\text{HC}]_1$  and  $[\text{HC}]_2$  are the concentrations of the hydrocarbon at time  $t_1$  and  $t_2$  respectively. The mean  $[\text{OH}]$  between  $t_1$  and  $t_2$  was calculated using Eq. (5):

$$[\text{OH}] = \frac{(k' - k_{\text{Dil}})}{k_{\text{OH}}}, \quad (5)$$

where  $k_{\text{Dil}}$  is the dilution rate of the measured [HC] due to continuous sampling from instrumentation (e.g. FAGE). Bloss et al. (2004) found the Guggenheim method to be most effective when smoothing the inferred  $[\text{OH}]$  over five [HC] measurements (i.e. consider 10 measurements taken at times  $t_1 - t_{10}$ ;  $[\text{OH}]$  at  $t_5$  would take  $[\text{HC}]_1$  and  $[\text{HC}]_5$ ,  $[\text{OH}]$  at  $t_6$  would take  $[\text{HC}]_2$  and  $[\text{HC}]_6$  etc.). Due to the short experiment time (20–30 min) and the 2–6 min time resolution on the GC measurements, this smoothing was not possible. For *iso*-butene, FTIR measurements were taken every 30 s, and these were typically found to be in excellent agreement with the GC-FID-measured HC decays, as shown in Fig. 5. However, measurement of small changes in the [HC], due to low steady-state  $[\text{OH}]$  in the chamber ( $\sim 5 \times 10^6 \text{ molecule cm}^{-3}$ ), led to large point-to-point variation in the inferred  $[\text{OH}]$ , even after the smoothing was applied. A solution was found by fitting the hydrocarbon decay data with an empirical exponential function of the form

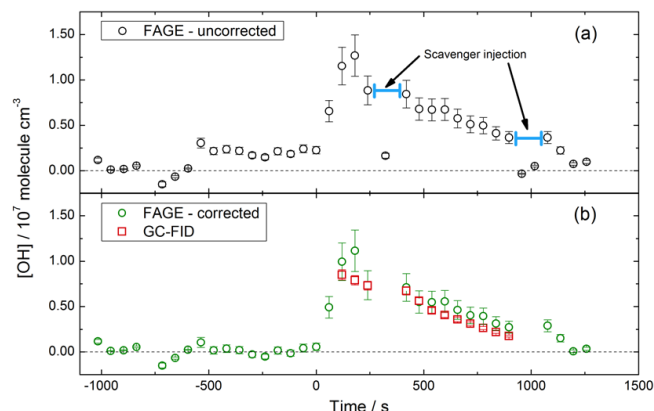


**Figure 6.** Comparison of [OH] traces measured using the HIRAC FAGE instrument (200 Hz PRF) during the photo-oxidation of *n*-pentane at 1000 mbar and 293 K before (a) and after (b), correcting for laser-generated OH due to TBHP photolysis in the OH fluorescence cell. The uncorrected and corrected FAGE signal was converted to [OH] using  $C_{\text{OH}} = 3.6 \times 10^{-8} \text{ counts cm}^3 \text{ s}^{-1} \text{ molecule}^{-1} \text{ mW}^{-1}$  determined using the conventional calibration method for comparison with GC-FID data. The TBHP ( $3.2 \times 10^{13} \text{ molecule cm}^{-3}$ ) and *n*-pentane ( $2.1 \times 10^{13} \text{ molecule cm}^{-3}$ ) were introduced into the chamber at  $t \approx -500 \text{ s}$ , and the photolysis lamps were switched on at  $t = 0 \text{ s}$ . The [OH] inferred from the HC decay method is also displayed in (b). Dashed line at  $y = 0$  given for clarity.

$y = A \times e^{(-x/t1)} + y_0$  as shown in Fig. 5, which allowed the accurate calculation of [HC] at the same time resolution as the FAGE instrument (20 s averaged). A negligible difference between inferred [OH] determined using the FTIR or GC-FID data was observed, and hence only GC-FID-measured hydrocarbon decays were used for direct comparison with *n*-pentane and cyclohexane.

Displayed in Fig. 6 is a typical [OH] profile for the photo-oxidation of *n*-pentane ( $2.1 \times 10^{13} \text{ molecule cm}^{-3}$ ) in HIRAC at 1000 mbar and 293 K where photolysis of TBHP was used to produce  $\sim 1.3 \times 10^7 \text{ molecule cm}^{-3}$  OH at  $t = 0$ . The OH was measured directly using the HIRAC FAGE instrument with the Litron Nd:YAG pumped dye laser light source, operating at 200 Hz PRF. Upon introduction of TBHP ( $3.2 \times 10^{13} \text{ molecule cm}^{-3}$ ) to the dark chamber at  $t \approx -500 \text{ s}$ , an OH signal equivalent to  $\sim 2.5 \times 10^6 \text{ molecule cm}^{-3}$  was observed, and was typically  $< 25 \%$  of the total detected OH signal following lamp photolysis. The measured un-normalised OH fluorescence signal was observed to increase quadratically with laser power, suggesting a two-photon photolysis-probe process from the OH probe laser at 308 nm, as described by Reactions (R5)–(R7).



This phenomenon was not observed during a brief test of the HIRAC FAGE instrument with a 5 kHz PRF laser system (JDSU Nd:YAG pumped Sirah Cobra Stretch dye laser, as in Glowacki et al., 2007a, and Malkin et al., 2010), most likely due to much lower laser pulse energies for the 5 kHz system ( $1.6 \mu\text{J pulse}^{-1}$  compared to  $40 \mu\text{J pulse}^{-1}$  at 200 Hz PRF). Using the scavenger injection system (Sect. 2.2), the decay of the TBHP could be accurately described (compared to simultaneous FTIR measurements) characterising the interference signal. At a time defined by the user, the *iso*-butane scavenger (20 % in  $\text{N}_2$ ) was injected into the FAGE cell for  $\sim 90 \text{ s}$  at  $\sim 20 \text{ sccm}$ . Before the chamber photolysis lamps were initiated, the OH interference signal was measured with the scavenger off and on, and the difference in signal was observed to be negligible (within the uncertainty of the measurement). The OH interference profile during the hydrocarbon decay was characterised and accounted for using 3–4 scavenger injections per experiment. An empirical fit to the averaged signals was used to correct the measured OH signal from TBHP laser photolysis over time, shown here in Fig. 6b compared to the inferred [OH] from the GC-FID. The type of fitting parameter (e.g. linear or exponential) was judged depending on the quality of data.

The calibration procedure was completed by plotting the OH signals, normalised for laser power, measured by FAGE as a function of the calculated OH concentrations from the hydrocarbon decays producing a calibration plot with  $C_{\text{OH}}$ , in units of  $\text{counts cm}^3 \text{ s}^{-1} \text{ mW}^{-1} \text{ molecule}^{-1}$ , as the gradient. A typical calibration plot is shown in Fig. 7 – produced using the decay of cyclohexane at 1000 mbar chamber pressure (see caption for detailed operating conditions). Uncertainties in  $C_{\text{OH}}$  are quoted to  $\pm 2\sigma$ , and error bars represent the standard error, and hence precision, of the measured  $S_{\text{OH}}$  to  $\pm 1\sigma$ . Error bars were kept at  $\pm 1\sigma$  as this represented the precision used in the analysis procedure.

## 4.2 Formaldehyde photolysis

Calibration of the  $\text{HO}_2$  detection cell required only the generation of  $\text{HO}_2$  radicals in the HIRAC chamber, and a time-dependent measurement of their subsequent recombination using the FAGE instrument once the photolysis lamps were extinguished. Upon photolysis in air (lamps: Philips TL40W/12 RS), HCHO produced  $\text{H} + \text{HCO}$  and  $\text{H}_2 + \text{CO}$  (Reaction R9) in approximately a 60 : 40 ratio (Reactions R8, R9). Under the conditions in HIRAC, HCO reacted with  $\text{O}_2$  to give  $\text{HO}_2 + \text{CO}$  (Reaction R10) and the H atom produced in Reaction (R8) reacted with  $\text{O}_2$  to give  $\text{HO}_2$  (Reaction R11). The loss of  $\text{HO}_2$  was characterised by the competing bimolecular and termolecular self-reactions (Reactions R12 + R13) and a first-order wall-loss parameter (Reaction R14):

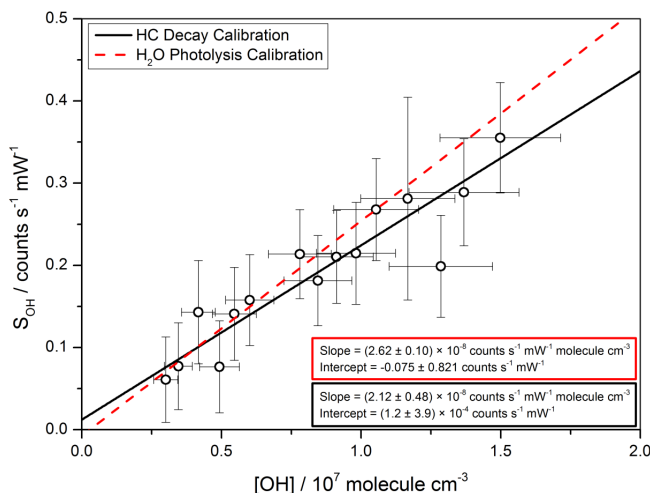
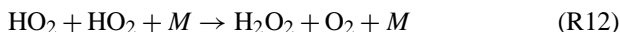


**Figure 7.** Calibration from the hydrocarbon decay method for cyclohexane at 1000 mbar and 293 K chamber pressure using the HIRAC FAGE instrument with the 200 Hz PRF laser system; inlet pressure =  $(3.81 \pm 0.02)$  mbar; laser power =  $(7.0 \pm 0.5)$  mW;  $[\text{H}_2\text{O}]_{\text{vapour}} < 10$  ppmv. Extrapolated calibration from the  $\text{H}_2\text{O}$  photolysis calibration technique for inlet pressure =  $(3.79 \pm 0.02)$  mbar, laser power =  $(6.0 \pm 0.5)$  mW,  $[\text{H}_2\text{O}]_{\text{vapour}} = (3900 \pm 20)$  ppmv and  $[\text{OH}] = (0.5\text{--}1.5) \times 10^9$  molecule  $\text{cm}^{-3}$ . Both fits are weighted to errors in the  $x$  and  $y$  axes and error bars are representative of the standard error in the measurement to  $\pm 2\sigma$ . Uncertainties quoted for the slope and intercept represent the precision of the calibration processes to  $\pm 2\sigma$ .



Therefore the rate of loss of  $\text{HO}_2$  is given by:

$$\frac{d[\text{HO}_2]}{dt} = -\left(k_{\text{loss}}[\text{HO}_2] + k_{\text{HO}_2 + \text{HO}_2}[\text{HO}_2]^2\right), \quad (6)$$

where  $k_{\text{HO}_2 + \text{HO}_2}$  is the  $\text{HO}_2$  recombination rate coefficient; the sum of the pressure-independent (Reaction R12) and pressure-dependent (Reaction R13) rate coefficients as determined by IUPAC (2007). Solving analytically for  $[\text{HO}_2]_t$  at a given time,  $t$ , integration of Eq. (5) becomes

$$\frac{1}{[\text{HO}_2]_t} = \left(\frac{1}{[\text{HO}_2]_0} + \frac{2 \cdot k_{\text{HO}_2 + \text{HO}_2}}{k_{\text{loss}}}\right) \times e^{(k_{\text{loss}}t)} - \left(\frac{2 \cdot k_{\text{HO}_2 + \text{HO}_2}}{k_{\text{loss}}}\right). \quad (7)$$

The  $[\text{HO}_2]$  in Eq. (6) is unknown but is related to the normalised  $\text{HO}_2$  signals measured by FAGE,  $S_{\text{HO}_2}$ , and the in-

strument sensitivity to  $\text{HO}_2$ ,  $C_{\text{HO}_2}$ , and therefore

$$\begin{aligned} (S_{\text{HO}_2})_t &= \left( \left( \frac{1}{(S_{\text{HO}_2})_0} + \frac{2 \cdot k_{\text{HO}_2 + \text{HO}_2}}{k_{\text{loss}} \cdot C_{\text{HO}_2}} \right) \right. \\ &\times e^{(k_{\text{loss}}t)} - \left. \left( \frac{2 \cdot k_{\text{HO}_2 + \text{HO}_2}}{k_{\text{loss}} \cdot C_{\text{HO}_2}} \right) \right)^{-1}, \quad (8) \end{aligned}$$

where  $(S_{\text{HO}_2})_t$  and  $(S_{\text{HO}_2})_0$  are the  $\text{HO}_2$  signal at time  $t$  and  $t = 0$  respectively.

The measured decay of  $S_{\text{HO}_2}$  using FAGE and the fit described by Eq. (7) are displayed in Fig. 8a for a typical experiment (aircraft FAGE instrument (5 kHz PRF), 1000 mbar, 298 K,  $< 10$  ppm  $[\text{H}_2\text{O}]$ , mixing fans on). Both  $k_{\text{loss}}$  and  $C_{\text{HO}_2}$  were determined by data fitting the  $S_{\text{HO}_2}$  decay using Eq. (7) with a Levenberg–Marquardt non-linear least-squares algorithm, fixing the initial signal and  $k_{\text{HO}_2 + \text{HO}_2}$ . The first  $\sim 100$  s of data were used, ensuring analysis after an almost complete decay of  $S_{\text{HO}_2}$ . Fitting was improved by the inclusion of upper and lower bounds of  $\pm 10\%$  for the  $(S_{\text{HO}_2})_0$  into the fitting routine, which accounted for the uncertainty in the determination of  $(S_{\text{HO}_2})_0$  (see Sect. 5.4.3).

For the experimental 350–1000 mbar pressure range at 0%  $\text{H}_2\text{O}$  vapour,  $k_{\text{HO}_2 + \text{HO}_2}$  was determined between  $(2.00\text{--}2.85) \times 10^{-12}$   $\text{cm}^3$  molecule $^{-1}$  s $^{-1}$ , according to the recommendation given by IUPAC (2007). A calibration was conducted at  $[\text{H}_2\text{O}]_{\text{vap}} = 7500$  ppmv, to validate the calibration method at high water vapour concentrations, representative of the conventional  $\text{H}_2\text{O}$  vapour photolysis method. The  $k_{\text{HO}_2 + \text{HO}_2}$  therefore included a correction for the  $\text{HO}_2\text{--H}_2\text{O}$  vapour chaperone effect (Stone and Rowley, 2005) in accordance with the IUPAC recommendation (Atkinson et al., 2004). The wall-loss rate,  $k_{\text{loss}}$ , was dependent on daily chamber conditions and was therefore determined as part of the fitting procedure along with  $C_{\text{HO}_2}$ , typically between 0.032 and 0.073 s $^{-1}$  with an uncertainty of  $\pm 10\%$  ( $2\sigma$ ). Variations in the wall-loss rates have implications for the uncertainty in  $C_{\text{HO}_2}$  derivation (Sect. 5.4).

## 5 Results and discussion

All results presented here were taken using the HIRAC FAGE instrument using Litron Nd:YAG pumped dye laser light source operating at 200 Hz PRF, unless otherwise stated. Tabulated data from the alternative calibration methods are displayed in the Supplement (Tables S1 and S2). All uncertainties displayed are quoted to  $\pm 2\sigma$  and all regressions shown are empirical, unless otherwise stated.

### 5.1 Conventional $\text{H}_2\text{O}$ vapour photolysis calibration

#### 5.1.1 $C_{\text{OH}}$ and $C_{\text{HO}_2}$ as a function of internal cell pressure

The FAGE instrument sensitivity to OH (Fig. 9, HIRAC FAGE only) and  $\text{HO}_2$  (Fig. 10, top) was determined as a

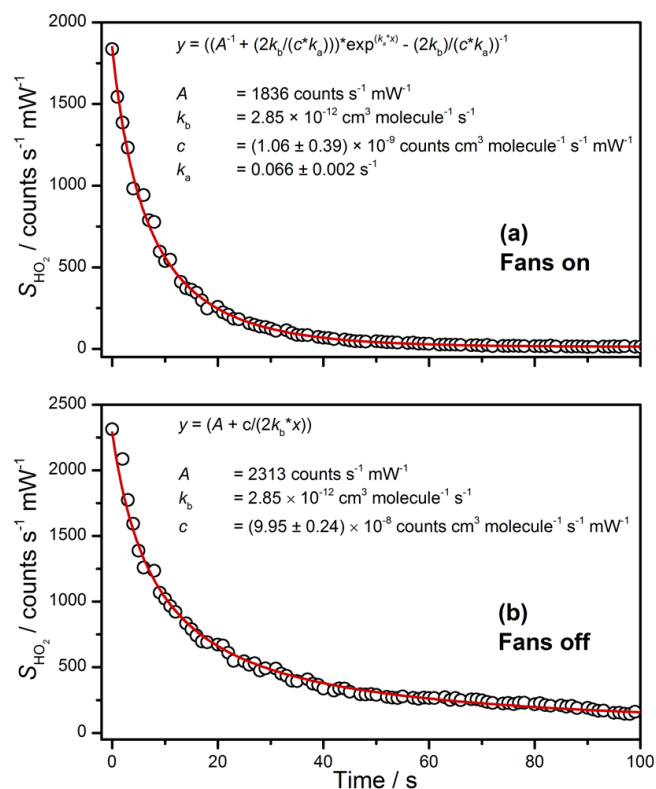


**Figure 8.** Normalised  $S_{\text{HO}_2}$  decay for the HCHO photolysis calibration method at 1000 mbar chamber pressure using the aircraft FAGE instrument (5 kHz PRF laser system) conducted with the HIRAC chamber mixing fans on (a) and off (b); inlet pressure =  $(2.53 \pm 0.02)$  mbar; laser power =  $(8.25 \pm 0.25)$  mW. Data in (a) were fitted with Eq. (7) to give  $C_{\text{HO}_2}$  where  $A = (S_{\text{HO}_2})_0$ ,  $k_b = k_{\text{HO}_2} + \text{HO}_2$ ,  $c = C_{\text{HO}_2}$ ,  $k_a = k_{\text{loss}}$  and  $z = \text{offset}$ , with uncertainties quoted to  $\pm 1\sigma$ . Parameters without quoted error were fixed.

function of pressure using the  $\text{H}_2\text{O}$  vapour photolysis calibration method over the inlet pressure range of 1.8–3.8 mbar. Figures 9 and 10 display the  $\text{H}_2\text{O}$  calibration data compared to those from the respective alternative calibration methods, the results for which are discussed in Sects. 5.2 and 5.3; error bars in both figures are representative of the total uncertainty in the calibration (Sect. 5.4 for details). Constant laser power and  $[\text{H}_2\text{O}]$  were maintained throughout the calibration process ( $8 \pm 1$  mW and  $4500 \pm 600$  ppmv respectively).

The linear regressions were used to describe the sensitivity as a function of fluorescence cell pressure for experiments conducted in HIRAC, and are a valid description of the data inside the 1.8–3.8 mbar pressure range only. The  $C_{\text{OH}}$  and  $C_{\text{HO}_2}$  data sets shown here were not conducted at the same time, but 6 months apart. This was due to the chronological order of the development of the alternative calibration techniques, during which time the FAGE pump set was serviced, increasing the pumping capacity and generally lowering the

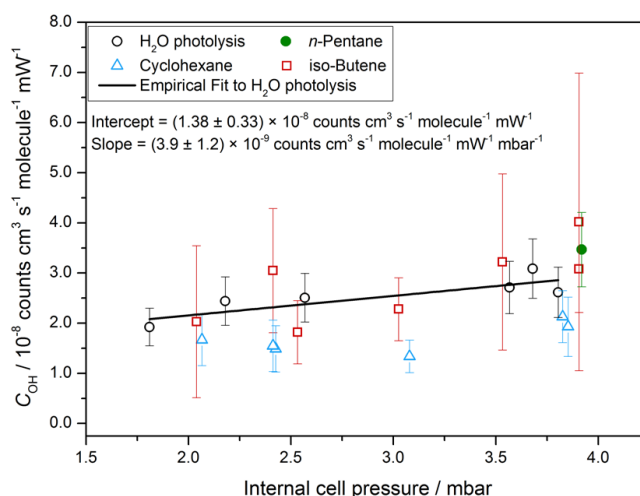


**Figure 9.** HIRAC FAGE instrument sensitivity to OH,  $C_{\text{OH}}$ , as a function of internal detection cell pressure as determined by the  $\text{H}_2\text{O}$  vapour photolysis and HC decay calibration techniques using the Litron Nd:YAG pumped dye laser operating at 200 Hz PRF. All calibrations were conducted at laser powers between 6.0 and 9.5 mW. Different internal cell pressures (1.8–3.8 mbar) were achieved by changing the diameter of the FAGE inlet pinhole between 0.5 and 1.0 mm. Conventional calibrations were conducted at constant  $[\text{H}_2\text{O}]_{\text{vap}}$  ( $4500 \pm 600$  ppmv), whereas alternative calibrations were conducted in near-dry conditions ( $< 15$  ppmv). HIRAC chamber pressures between 440 and 1000 mbar were used to induce internal cell pressures between 2.1 and 3.9 mbar. Error bars indicate the total uncertainty to  $\pm 1\sigma$ .

internal cell pressures for each pinhole in the  $C_{\text{OH}}$  determination.

The fit displayed a greater increase in  $C_{\text{HO}_2}$  as a function of pressure compared to  $C_{\text{OH}}$ , where  $\Delta C_{\text{OH}} = (17 \pm 11)\%$  and  $\Delta C_{\text{HO}_2} = (31.6 \pm 4.4)\%$  increase between 1.3 and 3.8 mbar. Altering the pinhole diameter could change the flow dynamics inside the instrument, reducing NO mixing efficiency, and therefore  $\text{HO}_2$  conversion efficiency, before the  $\text{HO}_2$  cell. The decrease in  $C_{\text{HO}_2}$  at lower pressure has been reproduced in a more recent calibration of the  $\text{HO}_2$  cell using the 5 kHz PRF laser source (slope =  $(5.14 \pm 0.46) \times 10^{-9}$  counts  $\text{cm}^3$  molecule $^{-1}$  s $^{-1}$  mW $^{-1}$  mbar $^{-1}$ ), suggesting the process was not affected by changes in laser pulse energy.

The experimental parameters controlling the instrument sensitivity,  $C_{\text{OH}}$ , which are dependent upon pressure, are the OH concentration in the laser-excitation region,  $[\text{OH}]_{\text{cell}}$ ; the fluorescence quantum yield following laser excitation to the OH  $\text{A}^2\Sigma^+$  ( $v' = 0$ ) excited state,  $\varphi_{\text{fl}}$ ; and the fraction of the fluorescence decay which falls within the integrating gate of the photon counter,  $f_{\text{gate}}$  (Creasey et al., 1997b; Faloon et al., 2004). The OH concentration in the cell held at total density  $[M]$  and the fluorescence quantum yield are given by

Eqs. (8) and (9):

$$[\text{OH}]_{\text{cell}} = \chi[M], \quad (9)$$

$$\varphi_{\text{fl}} = \frac{A}{(A + k_{\text{q}}[M])}, \quad (10)$$

where  $\chi$  is the mixing ratio of OH impinging at the pinhole (assuming no losses at the pinhole),  $A$  is the inverse of the radiative lifetime of OH and  $k_{\text{q}}$  is the rate coefficient for quenching of the excited  $A^2\Sigma^+$  ( $v' = 0$ ) (averaged appropriately over all quenching species). Assuming that  $f_{\text{gate}} = 1$ , then the overall pressure-dependent term for instrument sensitivity to OH can be described as the product of Eqs. (8) and (9), shown here in Eq. (10):

$$\varphi\chi[\text{OH}]_{\text{cell}} \times \Phi_{\text{fl}} = \frac{[M]A}{(A + k_{\text{q}}[M])}. \quad (11)$$

When  $[M] \rightarrow 0$ , the product becomes  $\chi[M]$ , and  $C_{\text{OH}}$  is directly proportional to pressure ( $[M]$ ). At higher pressures when  $k_{\text{q}}[M] \gg A$  (at 18 mbar the ratio is  $\sim 10$ ), the product becomes  $\sim \chi A/k_{\text{q}}$  and  $C_{\text{OH}}$  is independent of  $[M]$ , and thus depends only on the mixing ratio of OH.

However, FAGE is an on-resonance technique, and therefore it is not possible to achieve the limit  $f_{\text{gate}} = 1$ , because it is necessary to gate off the CPM during the laser pulse in order to avoid saturation of the detector. Thus, in these experiments  $f_{\text{gate}}$  was always  $< 1$ , and depended non-linearly on pressure because the photon-counting gate remained the same whilst the fraction of the total fluorescence collected within this gate ( $f_{\text{gate}}$ ) changed as a result of changes in the total fluorescence lifetime of the excited-state OH radicals. Thus the effective area of integration under the fluorescence decay curve reduced with increasing pressure such that  $f_{\text{gate}}$  reduced non-linearly as pressure increased. For the conditions used in these experiments  $f_{\text{gate}} = 0.79\text{--}0.63$  (between 1.3 and 3.8 mbar). Hence the observation that  $C_{\text{OH}}$  increased linearly over pressures between 1.3 and 3.8 mbar in this study is consistent with the expected behaviour based purely on the balance between OH number density and the total fluorescence collected.

The inherent complexity that results from the multiple factors which control the sensitivity of FAGE instruments, and which also change with a variety of conditions (i.e. pressure,  $[\text{H}_2\text{O}]$ , laser power) and instrumental factors (e.g. time take for CPM to reach maximum gain), require that FAGE instruments are frequently and carefully calibrated.

Additional investigations into the FAGE instrument sensitivity to OH as a function of  $[\text{H}_2\text{O}]_{\text{vap}}$  and laser power are discussed in detail in the Supplement. The change in instrument sensitivity over  $[\text{H}_2\text{O}]$  between 200 and 4500 ppmv was observed to be within the uncertainty of the calibration (35 % at  $2\sigma$ ) and was therefore considered negligible. For this reason no correction for sensitivity to  $[\text{H}_2\text{O}]$  was applied to the data taken in the alternative calibration method where  $[\text{H}_2\text{O}] < 10$  ppmv.

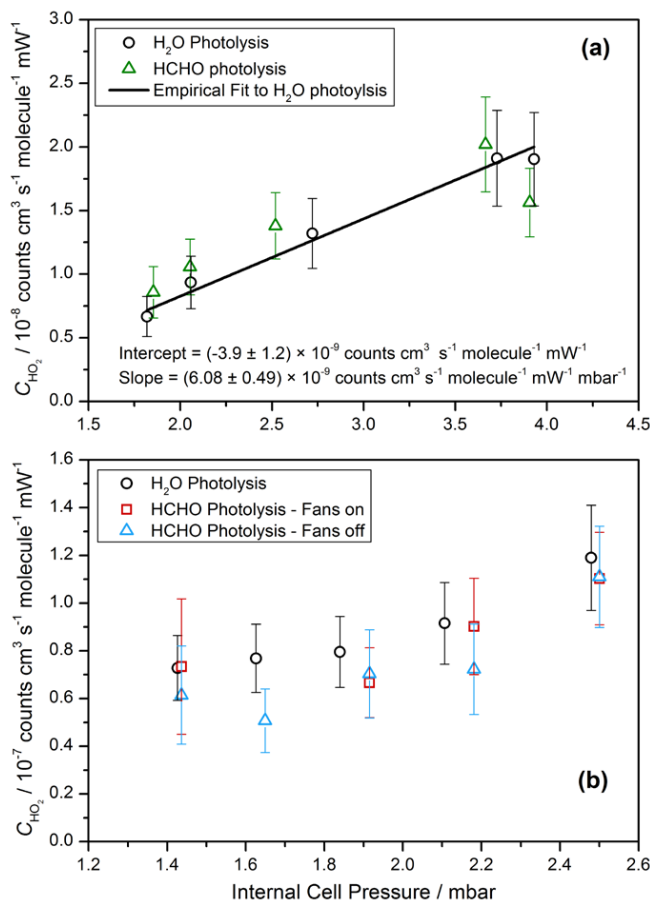


**Figure 10.** FAGE instrument sensitivity to  $\text{HO}_2$ ,  $\text{C}_{\text{HO}_2}$ , as a function of internal detection cell pressure as determined by the  $\text{H}_2\text{O}$  vapour and HCHO photolysis calibration techniques using the HIRAC FAGE instrument operating at 200 Hz PRF (a) and the aircraft FAGE instrument operating at 5 kHz PRF (b). Conventional calibrations were conducted at constant  $[\text{H}_2\text{O}]_{\text{vap}}$  ((a)  $4500 \pm 600$  ppmv, (b)  $6000 \pm 600$  ppmv), whereas alternative calibrations were conducted under low  $[\text{H}_2\text{O}]_{\text{vap}}$  ( $< 15$  ppmv). HIRAC chamber pressures of 440–1000 mbar were used to induce internal cell pressures of (a) 1.8–3.8 mbar (pinhole diameter 0.5–1.0 mbar) and (b) 1.42–2.48 mbar (pinhole diameter 0.3–0.6 mbar). Error bars indicate the total uncertainty to  $\pm 1\sigma$ .

## 5.2 Hydrocarbon decay calibration

Figure 7 shows a direct comparison of analysed data from the decay of cyclohexane and  $\text{H}_2\text{O}$  vapour calibration method at  $\sim 3.80$  mbar internal cell pressure (equivalent to 1000 mbar in HIRAC) using the 1.0 mm inlet pinhole and  $\sim 7$  mW laser power. The  $C_{\text{OH}}$  was determined as  $(2.13 \pm 0.52) \times 10^{-8}$  counts  $\text{s}^{-1}$  molecule $^{-1}$   $\text{cm}^3$   $\text{mW}^{-1}$ , within error of the traditional  $\text{H}_2\text{O}$  vapour photolysis calibration ( $2\sigma$ ) at the same pressure ( $(2.62 \pm 0.91) \times 10^{-8}$  counts  $\text{s}^{-1}$  molecule $^{-1}$   $\text{cm}^3$   $\text{mW}^{-1}$ ). Error bars are representative of the total uncertainty at  $\pm 1\sigma$ . Additional example calibration plots for each hydrocarbon

studied are included in the Supplement. Displayed in Fig. 9 is  $C_{\text{OH}}$  as a function of internal cell pressure using the HC decay calibration method, determined for *iso*-butene, cyclohexane and *n*-pentane. The HC decay calibration method was observed to be in agreement with the  $\text{H}_2\text{O}$  vapour photolysis calibration. The average of the ratio of calibration factors (conventional: alternative) was calculated for each alternative calibration point across the entire pressure range,  $C_{\text{OH}(\text{conv})}/C_{\text{OH}(\text{alt})} = 1.19 \pm 0.26$ , where  $C_{\text{OH}(\text{conv})}$  was determined from the fit to the  $\text{H}_2\text{O}$  photolysis data.

A large variability in the  $C_{\text{OH}}$  determined using the *iso*-butene decay was observed, with larger uncertainties associated with this calibration compared to cyclohexane and *n*-pentane, and the reason for this remains unclear. On average, the measured OH signals were closer to the detection limit of the FAGE instrument when using *iso*-butene. Initial concentrations of each of the hydrocarbons were  $2.5 \times 10^{13}$  molecule  $\text{cm}^{-3}$ , and hence a lower OH steady-state concentration is expected when *iso*-butene is present as the  $k_{\text{OH}}$  is an order of magnitude higher than those for *n*-pentane and cyclohexane. As  $S_{\text{OH}}$  approaches 0 counts  $\text{s}^{-1}$   $\text{mW}^{-1}$ , the  $S_{\text{OH}}$  measurement becomes increasingly imprecise, and thus the uncertainty in the fitting of the calibration plot increases.

A general under-prediction of  $C_{\text{OH}}$ , compared to the  $\text{H}_2\text{O}$  vapour photolysis method, was observed when calculated using the decay of cyclohexane,  $C_{\text{OH}(\text{conv})}/C_{\text{OH}(\text{Chex})} = 1.52 \pm 0.44$ . The exact reason is unknown. Evaluation of the HC decay data with the  $k_{\text{OH}}$  adjusted at the upper limit of uncertainty recommended by Calvert et al. (2008) (25% ( $2\sigma$ ),  $k_{\text{OH}} = 8.04 \times 10^{-12}$   $\text{cm}^3$  molecule $^{-1}$   $\text{s}^{-1}$ ) brings the two data sets into better agreement,  $C_{\text{OH}(\text{conv})}/C_{\text{OH}(\text{Chex})} = 1.21 \pm 0.22$ . The cyclohexane measurements were also affected to a greater extent by the chamber dilution due to the slower rate of reaction with OH, which contributed to 25–30% of the total cyclohexane decay rate directly after the photolysis lamps were initiated, compared to 5–10% for the *iso*-butene experiments. Correcting the cyclohexane data for a hypothetically enhanced chamber dilution could explain the lower sensitivity measurements (as the decay increases,  $[\text{OH}]_{\text{inf}}$  increases), however the dilution rate was confirmed prior to photolysis of TBHP in each experiment.

### 5.3 Formaldehyde photolysis calibration

Figure 10a shows the instrument sensitivity to  $\text{HO}_2$ ,  $C_{\text{HO}_2}$ , as a function of internal cell pressure for the newly developed formaldehyde photolysis calibration technique for the HIRAC FAGE instrument. Each data point corresponds to the average of up to five  $\text{HO}_2$  decay traces (Fig. 8a), and the error bars are representative of the total calibration  $1\sigma$  uncertainty (Sect. 5.4). All calibrations were completed over a 4–8 mW laser power range. The alternative calibration was observed to be in good agreement with

the conventional  $\text{H}_2\text{O}$  vapour photolysis calibration technique over the operating internal cell pressure range of 1.8–3.8 mbar ( $C_{\text{HO}_2(\text{conv})}/C_{\text{HO}_2(\text{alt})} = 0.96 \pm 0.09$ ) for the Litron-based FAGE system.

The kinetics of the  $\text{HO}_2$  decay due to recombination and first-order wall loss (Eq. 7) were confirmed by studying the  $\text{HO}_2$  decay profile with the chamber mixing fans on and off using the University of Leeds aircraft-based FAGE instrument. With the mixing fans off, the decay was accurately described by the recombination kinetics only (Fig. 8b), giving  $C_{\text{HO}_2}$  values within error of the fans on experiments, as shown in Fig. 10b. Good agreement between the conventional and alternative calibration methods was also observed across the 1.42–2.48 mbar internal cell pressure range, and the overall correlation between conventional and alternative calibration methods was calculated as  $C_{\text{HO}_2(\text{conv})}/C_{\text{HO}_2(\text{alt})} = 1.07 \pm 0.09$  for the high-frequency aircraft-based FAGE instrument.

### 5.4 Calibration uncertainties

The overall uncertainty associated with the calibration methods presented here was calculated using the sum in quadrature of the accuracy and the precision terms of the calibration. The accuracy term accounted for any systematic uncertainty in the calculation of  $[\text{HO}_x]$  for each calibration method, signal normalisation etc., and these are displayed in Table 2. The precision of the calibrations was defined as the random errors associated with each method. All uncertainties are quoted as  $2\sigma$ .

#### 5.4.1 $\text{H}_2\text{O}$ photolysis calibration

The total uncertainty in the  $\text{H}_2\text{O}$  photolysis calibration method was estimated to be  $\sim 36\%$ . The accuracy was defined by the uncertainty associated with each term of Eq. (1) in the determination of  $[\text{HO}_x]$  and was estimated to be  $\sim 35\%$ . The largest contribution to the accuracy of this calibration method came from the determination of the calibration source flux,  $F_{184.9\text{nm}}$ , with a total uncertainty of 32%. The product of the flux and the irradiation time from Eq. (1),  $F_{184.9\text{nm}} \times \Delta t$ , was determined using  $\text{N}_2\text{O}$  actinometry which relied on the detection of trace levels of NO (0.5–3 ppbv, Sect. 2.1) followed by evaluation of the measurements using four rate constants each with  $\sim 20\%$  uncertainty. Although the actinometric method gives a direct determination of the product  $F_{184.9\text{nm}} \times \Delta t$ , in order to calculate  $[\text{OH}]$  from Eq. (1) any differences between the total volumetric flow rate during the actinometry experiment and the OH calibration needs to be accounted for as they change  $\Delta t$ . It is therefore necessary to account for the uncertainty in  $\Delta t$ , which was determined to be  $\sim 2\%$  using the uncertainty in the flow rates from the mass flow controllers ( $\sim 1\%$ ). For the remainder of the terms in Eq. (1) their contributions to the accuracy in the  $\text{H}_2\text{O}$  photolysis calibration method were

**Table 2.** The systematic uncertainties to  $2\sigma$  in the various parameters that determine the accuracy in the OH and HO<sub>2</sub> calibration factors for all three calibration methods. Total accuracy is taken as the sum in quadrature of the individual uncertainties. The Online position error is the approximate error in the maximum line intensity that is achieved when positioning the laser wavelength at the centre of the OH transition.

H <sub>2</sub> O + $h\nu$		Hydrocarbon decay		HCHO + $h\nu$	
Parameter	Uncertainty	Parameter	Uncertainty	Parameter	Uncertainty
$F_{184.9\text{nm}}$	32 %	$k_{\text{OH}}$	20–25 %	$k_{\text{HO}_2+\text{HO}_2}$	35 %
$\Delta t$	2 %	$k_{\text{Dil}}$	10 %	$S_{\text{HO}_2}$ initial	20 %
[H <sub>2</sub> O]	10 %	GC-FID	4 %	Laser power	6 %
$\sigma_{\text{H}_2\text{O},184.9\text{nm}}$	6 %	Laser power	6 %	Online position	4 %
Laser power	6 %	Online position	4 %		
Online position	4 %				
Error	35 %	Error	24–28 %	Error	41 %

as follows:  $\sigma_{\text{H}_2\text{O}}$  was taken from Cantrell et al. (1997), with a reported total error of  $\pm 6\%$ ; the error in [H<sub>2</sub>O] was taken from the hygrometer instrumental uncertainty ( $\pm 10\%$ ); and laser power was defined by the laser power meter (Molelectron Powermax 500A,  $\pm 0.25$  mW).

The precision was typically between 4 and 10 % for the flow tube calibration process and was taken from the standard error in the error-weighted fit of the calibration plot. The error bars were representative of the standard deviation in the  $S_{\text{OH}}$  and [HO<sub>*x*</sub>] for the *x* and *y* axes respectively. The flux output of the calibration source, hygrometer and CPM measurements were observed to have good point-to-point stability and therefore low standard deviations.

#### 5.4.2 Hydrocarbon decay calibration

The accuracy of the hydrocarbon decay method was estimated to be better than that of the flow tube method ( $\sim 28\%$  compared to 35 %). However, due to the large variation in the random errors that defined the precision of the experiment, the total uncertainty for the HC decay method was larger than the flow tube calibration method, with the total uncertainty estimated at  $\sim 45\%$ .

The accuracy in the calibration was intrinsic to the hydrocarbon used, being dependent on the uncertainty in  $k_{\text{OH}}$  and  $k_{\text{Dil}}$ . The largest uncertainty was in  $k_{\text{OH}}$ , taken from data reviews from the Calvert series or IUPAC recommendations: *n*-pentane,  $\pm 20\%$  (Calvert et al., 2008); cyclohexane,  $\pm 20\%$  (Calvert et al., 2008); and *iso*-butene,  $\pm 25\%$  (IUPAC, 2007). Uncertainty in  $k_{\text{Dil}}$  was calculated from repeated measurements of chamber dilution for each of the hydrocarbons, and induced errors in GC-FID calibration (4 %). The precision of the experiments for both *n*-pentane and cyclohexane was between 10 and 25 %, whereas *iso*-butene showed much greater variation of between 13 and 69 %; possible reasons for this have been discussed in Sect. 5.2.

#### 5.4.3 Formaldehyde photolysis calibration

The total uncertainty for the HCHO photolysis calibration method has been estimated at  $\sim 46\%$ , which is 10 % greater than the conventional calibration method. The accuracy of the HCHO photolysis method was estimated as  $\sim 41\%$ ; the largest contribution to this deriving from the uncertainty was in the HO<sub>2</sub> recombination rate constant (35 %), taken from the IUPAC recommendation (IUPAC, 2007). Determining the accurate initial  $S_{\text{HO}_2}$  (i.e.  $S_{\text{HO}_2}$  at  $t_0$ ) is hard as HO<sub>2</sub> does not fully reach steady state before the photolysis lamps are switched off; therefore there is a certain amount of subjective choice in the value of  $S(\text{HO}_2)_0$ , and hence the uncertainty in the initial  $S_{\text{HO}_2}$  was based on the standard deviation of the mean “steady-state” HO<sub>2</sub> signal, which gives an estimation of the 1 s point-to-point variability for a chosen  $t_0$  ( $\sim 20\%$ ).

The error associated with the precision of the experiment was taken from the error propagation of the standard error terms from the Levenberg–Marquardt iterative fitting procedure for Eq. (9) and Fig. 8. This includes both the error in the  $C_{\text{HO}_2}$  and  $k_{\text{loss}}$  parameters. The precision for this method was in line with the conventional flow tube calibration between 10 and 20 %.

## 6 Conclusions and outlook

The first pressure-dependent calibrations of a FAGE instrument for both OH and HO<sub>2</sub> have been successfully conducted using the HIRAC chamber. Previous pressure-dependent aircraft measurements had been extracted by assuming that the calibration factor could be determined by simply calibrating at the required internal FAGE cell pressure. Assumptions were therefore made that variations in radical losses on the inlet and the nature of the expansion caused by the varying pressure differential inside and outside the FAGE cell were insignificant. The results displayed in Figs. 9 and 10 validate the conventional calibration method with the alternative hydrocarbon decay and HCHO photolysis methods over a range of internal FAGE cell pressures. It should be emphasised that,

strictly speaking, this validation applies only to these particular FAGE instruments, but this work suggests that the agreement between the different calibration techniques will translate to FAGE instruments of similar designs. As the calibration methods are quite different in principle, they are unlikely to be subject to the same systematic errors. The alternative calibration results presented here have been shown to be well within the combined uncertainty of their respective traditional calibration method, validating the pressure-dependent flow tube calibration technique and improving confidence in FAGE measurements both in the field and in kinetics experiments. Both alternative methods have also shown that calibrations conducted under high  $[\text{H}_2\text{O}]_{\text{vap}}$  conditions (2000–4500 ppmv) can be applied to measurements at low  $[\text{H}_2\text{O}]_{\text{vap}}$  ( $< 15$  ppmv).

The hydrocarbon decay method has shown that the FAGE instrument can be calibrated over a range of external pressures using different hydrocarbons. Compared to the conventional calibration method, where  $[\text{HO}_x]$  are generated typically at  $> 10^8$  molecule  $\text{cm}^{-3}$ , the hydrocarbon decay method is conducted at a  $[\text{HO}_x]$  relevant to chamber-based experimental measurements ( $\sim 10^7$  molecule  $\text{cm}^{-3}$ ) and much closer to typical ambient OH concentrations ( $\sim 10^6$  molecule  $\text{cm}^{-3}$ ).

Currently the total error associated with the hydrocarbon decay method is greater than that of the flow tube method ( $\sim 45\%$  vs.  $36\%$ ). The accuracy or total systematic uncertainty associated with the alternative OH calibration method is lower than that of the flow tube calibration method ( $28\%$  vs.  $35\%$ ), and hence an improvement in the precision of the experiment could improve the overall uncertainty to be in line with the flow tube method. The primary source of random error arose in the detection of OH close to the detection limit. Increasing the steady-state OH concentration in the chamber would allow easier detection of the hydrocarbon decay compared to chamber dilution, as well as an OH measurement above the detection limit. The steady-state OH concentration could be increased by increasing the 254 nm intensity in the chamber; using new lamps or more lamps; altering the OH precursor, e.g.  $\text{O}_3$ + alkenes or photolysis of methyl nitrite; or by lowering the initial [HC]. The latter would require a more sensitive hydrocarbon detection technique than GC-FID or FTIR, which are currently available in HIRAC. One such technique is proton transfer mass spectrometry (PTR-MS), which would reduce the uncertainty in the hydrocarbon decay measurements by providing higher-time-resolution measurements and allow for easier simultaneous measurement of multiple hydrocarbons at low concentrations, effectively providing multiple independent estimates of  $C_{\text{OH}}$  from a single experiment. Uncertainties in the rate coefficients could also be reduced by a concerted laboratory study including relative rate and direct flash photolysis methods, decreasing the systematic error. With careful experimental design, errors could potentially be reduced to closer

to  $10\%$  (Orkin et al., 2010; Carr et al., 2011; Glowacki et al., 2012).

A full range of pressure-dependent calibrations using this method would currently take  $\sim 2$  days, compared to  $\sim 3$  h for the flow-tube-based calibration. However, the timescale does not limit the suitability of the method for regular confirmation of  $C_{\text{OH}}$  obtained from the flow tube calibration method.

The total uncertainty in the HCHO photolysis method is  $\sim 46\%$  which is  $10\%$  greater than that of the traditional  $\text{H}_2\text{O}$  photolysis method. The HCHO photolysis method is quick and reproducible. The time taken to complete the analysis and the errors is comparable with the flow tube technique. An advantage of the HCHO photolysis method is that several runs can be completed in one fill of the chamber, compared to the HC decay method, which requires one fill per experiment (although the proposed use of multiple HC decays will provide multiple estimates of  $C_{\text{OH}}$  from a single chamber fill).

**The Supplement related to this article is available online at doi:10.5194/amt-8-523-2015-supplement.**

*Acknowledgements.* This work was supported by funding from the Natural Environment Research Council (NERC grant NE/G523739/1), EUROCHAMP-2 and the National Centre for Atmospheric Science (NCAS). I. Bejan acknowledges a Marie Curie fellowship. We are grateful for helpful discussions with Andrew Goddard and Mark Blitz on technical aspects of HIRAC and lasers respectively.

Edited by: A. Hofzumahaus

## References

- Aschmutat, U., Hessling, M., Holland, F., and Hofzumahaus, A.: A tunable source of Hydroxyl (OH) and Hydroperoxy ( $\text{HO}_2$ ) radicals: in the range between  $10^6$  and  $10^9$   $\text{cm}^{-3}$ , in: *Physico-Chemical Behaviour of Atmospheric Pollutants*, edited by: Restelli, G. A. a. G., European Commission, Brussels, 811–816, 1994.
- Atkinson, R.: Kinetics and mechanisms of the gas-phase reactions of the hydroxyl radical with organic compounds under atmospheric conditions, *Chem. Rev.*, 86, 69–201, 1986.
- Atkinson, R.: Gas-phase tropospheric chemistry of organic compounds, *J. Phys. Chem. Ref. Data. Mono.*, 2, 1994.
- Atkinson, R.: Kinetics of the gas-phase reactions of OH radicals with alkanes and cycloalkanes, *Atmos. Chem. Phys.*, 3, 2233–2307, doi:10.5194/acp-3-2233-2003, 2003.
- Atkinson, R. and Pitts, J. N. J.: Rate Constants for the Reaction of OH Radicals with Propylene and the Butenes over the Temperature Range 297–425 K, *J. Chem. Phys.*, 63, 3591–3595, 1975.
- Atkinson, R., Baulch, D. L., Cox, R. A., Crowley, J. N., Hampson, R. F., Hynes, R. G., Jenkin, M. E., Rossi, M. J., and Troe, J.:

- Evaluated kinetic and photochemical data for atmospheric chemistry: Volume I – gas phase reactions of O<sub>x</sub>, HO<sub>x</sub>, NO<sub>x</sub> and SO<sub>x</sub> species, *Atmos. Chem. Phys.*, 4, 1461–1738, doi:10.5194/acp-4-1461-2004, 2004.
- Baasandorj, M., Papanastasiou, D. K., Talukdar, R. K., Hasson, A. S., and Burkholder, J. B.: (CH<sub>3</sub>)<sub>3</sub>COOH (tert-butyl hydroperoxide): OH reaction rate coefficients between 206 and 375 K and the OH photolysis quantum yield at 248 nm, *Phys. Chem. Chem. Phys.*, 12, 12101–12111, doi:10.1039/c0cp00463d, 2010.
- Berresheim, H., Elste, T., Tremmel, H. G., Allen, A. G., Hansson, H. C., Rosman, K., Dal Maso, M., Makela, J. M., Kulmala, M., and O'Dowd, C. D.: Gas-aerosol relationships of H<sub>2</sub>SO<sub>4</sub>, MSA, and OH: Observations in the coastal marine boundary layer at Mace Head, Ireland, *J. Geophys. Res.-Atmos.*, 107, 8100, doi:10.1029/2000JD000229, 2002.
- Bloss, W. J., Lee, J. D., Bloss, C., Heard, D. E., Pilling, M. J., Wirtz, K., Martin-Reviejo, M., and Siese, M.: Validation of the calibration of a laser-induced fluorescence instrument for the measurement of OH radicals in the atmosphere, *Atmos. Chem. Phys.*, 4, 571–583, doi:10.5194/acp-4-571-2004, 2004.
- Brauers, T., Aschmutat, U., Brandenburger, U., Dorn, H. P., Hausmann, M., Hessling, M., Hofzumahaus, A., Holland, F., Plass-Dulmer, C., and Ehhalt, D. H.: Intercomparison of tropospheric OH radical measurements by multiple folded long-path laser absorption and laser induced fluorescence, *Geophys. Res. Lett.*, 23, 2545–2548, 1996.
- Calvert, J. G., Atkinson, R., Kerr, J. A., Madronich, S., Moortgat, G. K., Wallington, T. J., and Yarwood, G.: *The Mechanism of Atmospheric Oxidation of the Alkenes*, OUP, Oxford, 2000.
- Calvert, J. G., Derwent, R. G., Orlando, J. J., Tyndall, G. S., and Wallington, T. J.: *Mechanisms of Atmospheric Oxidation of the Alkanes*, Oxford University Press, 2008.
- Campuzano-Jost, P., Williams, M. B., D'Ottone, L., and Hynes, A. J.: Kinetics and mechanism of the reaction of the hydroxyl radical with h(8)-isoprene and d(8)-isoprene: Isoprene absorption cross sections, rate coefficients, and the mechanism of hydroperoxyl radical production, *J. Phys. Chem. A*, 108, 1537–1551, doi:10.1021/jp0363601, 2004.
- Cantrell, C. A., Tyndall, G., and Zimmer, A.: Absorption cross sections for water vapour from 183 to 193 nm, *Geophys. Res. Lett.*, 24, 2195–2198, 1997.
- Carr, S. A., Blitz, M. A., and Seakins, P. W.: Site-Specific Rate Coefficients for Reaction of OH with Ethanol from 298 to 900 K, *J. Phys. Chem. A*, 115, 3335–3345, doi:10.1021/jp200186t, 2011.
- Commane, R., Floquet, C. F. A., Ingham, T., Stone, D., Evans, M. J., and Heard, D. E.: Observations of OH and HO<sub>2</sub> radicals over West Africa, *Atmos. Chem. Phys.*, 10, 8783–8801, doi:10.5194/acp-10-8783-2010, 2010.
- Creasey, D. J., Halford-Maw, P. A., Heard, D. E., Pilling, M. J., and Whitaker, B. J.: Implementation and initial deployment of a field instrument for measurement of OH and HO<sub>2</sub> in the troposphere by laser-induced fluorescence, *J. Chem. Soc.-Faraday Trans.*, 93, 2907–2913, 1997a.
- Creasey, D. J., Heard, D. E., Pilling, M. J., Whitaker, B. J., Berzins, M., and Fairlie, R.: Visualisation of a supersonic free-jet expansion using laser-induced fluorescence spectroscopy: Application to the measurement of rate constants at ultralow temperatures, *Appl. Phys. B-Lasers Opt.*, 65, 375–391, 1997b.
- Creasey, D. J., Heard, D. E., and Lee, J. D.: Absorption cross-section measurements of water vapour and oxygen at 185 nm. Implications for the calibration of field instruments to measure OH, HO<sub>2</sub> and RO<sub>2</sub> radicals, *Geophys. Res. Lett.*, 27, 1651–1654, doi:10.1029/1999gl011014, 2000.
- Davis, D. D., Heaps, W., and McGee, T.: Direct Measurements of Natural Tropospheric Levels of OH *via* an Aircraft Borne Tunable Dye-Laser, *Geophys. Res. Lett.*, 3, 331–333, 1976.
- Dorn, H. P., Brandenburger, U., Brauers, T., Hausmann, M., and Ehhalt, D. H.: In-situ detection of tropospheric OH radicals by folded long-path laser absorption, Results from the POPCORN field campaign in August 1994, *Geophys. Res. Lett.*, 23, 2537–2540, doi:10.1029/96gl02206, 1996.
- Dusanter, S., Vimal, D., and Stevens, P. S.: Technical note: Measuring tropospheric OH and HO<sub>2</sub> by laser-induced fluorescence at low pressure. A comparison of calibration techniques, *Atmos. Chem. Phys.*, 8, 321–340, doi:10.5194/acp-8-321-2008, 2008.
- Edwards, G. D., Cantrell, C., Stephens, S., Hill, B., Goyea, O., Shetter, R., Mauldin, R. L., Kosciuch, E., Tanner, D., and Eisele, F.: Chemical Ionization Mass Spectrometer Instrument for the Measurement of Tropospheric HO<sub>2</sub> and RO<sub>2</sub>, *Anal. Chem.*, 75, 5317–5327, 2003.
- Eisele, F. L. and Tanner, D. J.: Ion-Assisted Tropospheric OH Measurements, *J. Geophys. Res.-Atmos.*, 96, 9295–9308, 1991.
- Eisele, F. L., Mauldin, L., Cantrell, C., Zondlo, M., Apel, E., Fried, A., Walega, J., Shetter, R., Lefer, B., Flocke, F., Weinheimer, A., Avery, M., Vay, S., G., S., Podolske, J., Diskin, G., Barrick, J. D., Singh, H. B., Brune, W., Harder, H., Martinez, M., Bandy, A., Thornton, D., Heikes, B., Kondo, Y., Riemer, D., Sandholm, S., Tan, D., Talbot, R., and Dibb, J.: Summary of measurement intercomparisons during TRACE-P, *J. Geophys. Res.*, 108, 8791–8810, 2003.
- Eisele, F. L., Mauldin, R. L., Tanner, D. J., Cantrell, C., Kosciuch, E., Nowak, J. B., Brune, B., Faloona, I., Tan, D., Davis, D. D., Wang, L., and Chen, G.: Relationship between OH measurements on two different NASA aircraft during PEM Tropics B, *J. Geophys. Res.-Atmos.*, 106, 32683–32689, 2001.
- Faloona, I., Tan, D., Brune, W. H., Jaegle, L., Jacob, D. J., Kondo, Y., Koike, M., Chatfield, R., Poeschel, R., Ferry, G., Sachse, G., Vay, S., Anderson, B., Hannon, J., and Fuelberg, H.: Observations of HO<sub>x</sub> and its relationship with NO<sub>x</sub> in the upper troposphere during SONEX, *J. Geophys. Res.-Atmos.*, 105, 3771–3783, 2000.
- Faloona, I. C., Tan, D., Leshner, R. L., Hazen, N. L., Frame, C. L., Simpas, J. B., Harder, H., Martinez, M., Di Carlo, P., Ren, X. R., and Brune, W. H.: A laser-induced fluorescence instrument for detecting tropospheric OH and HO<sub>2</sub>: Characteristics and calibration, *J. Atmos. Chem.*, 47, 139–167, doi:10.1023/B:JOCH.0000021036.53185.0e, 2004.
- Fuchs, H., Bohn, B., Hofzumahaus, A., Holland, F., Lu, K. D., Nehr, S., Rohrer, F., and Wahner, A.: Detection of HO<sub>2</sub> by laser-induced fluorescence: calibration and interferences from RO<sub>2</sub> radicals, *Atmos. Meas. Tech.*, 4, 1209–1225, doi:10.5194/amt-4-1209-2011, 2011.
- Fuchs, H., Dorn, H.-P., Bachner, M., Bohn, B., Brauers, T., Gomm, S., Hofzumahaus, A., Holland, F., Nehr, S., Rohrer, F., Tillmann, R., and Wahner, A.: Comparison of OH concentration measurements by DOAS and LIF during SAPHIR chamber experiments

- at high OH reactivity and low NO concentration, *Atmos. Meas. Tech.*, 5, 1611–1626, doi:10.5194/amt-5-1611-2012, 2012.
- Glowacki, D. R., Goddard, A., Hemavibool, K., Malkin, T. L., Commane, R., Anderson, F., Bloss, W. J., Heard, D. E., Ingham, T., Pilling, M. J., and Seakins, P. W.: Design of and initial results from a Highly Instrumented Reactor for Atmospheric Chemistry (HIRAC), *Atmos. Chem. Phys.*, 7, 5371–5390, doi:10.5194/acp-7-5371-2007, 2007a.
- Glowacki, D. R., Goddard, A., and Seakins, P. W.: Design and performance of a throughput-matched, zero-geometric-loss, modified three objective multipass matrix system for FTIR spectrometry, *Appl. Opt.*, 46, 7872–7883, doi:10.1364/ao.46.007872, 2007b.
- Glowacki, D. R., Lockhart, J., Blitz, M. A., Klippenstein, S. J., Pilling, M. J., Robertson, S. H., and Seakins, P. W.: Interception of excited vibrational quantum states by O<sub>2</sub> in atmospheric association reactions, *Science (Washington, D.C., 1883)*, 337, 1066–1067, doi:10.1126/science.1224106, 2012.
- Guggenheim, E. A.: On the determination of the Velocity Constant of a Unimolecular Reaction, *Philos. Mag.*, 2, 538–543, 1926.
- Hard, T. M., George, L. A., and O'Brien, R. J.: FAGE Determination of Tropospheric HO and HO<sub>2</sub>, *J. Atmos. Sci.*, 52, 3354–3372, 1995.
- Heard, D. E.: Atmospheric field measurements of the hydroxyl radical using laser-induced fluorescence spectroscopy, *Ann. Rev. Phys. Chem.*, 57, 191–216, doi:10.1146/annurev.physchem.57.032905.104516, 2006.
- Heard, D. E. and Pilling, M. J.: Measurement of OH and HO<sub>2</sub> in the Troposphere, *Chem. Rev.*, 103, 5163–5198, 2003.
- Hofzumahaus, A., Brauers, T., Aschmutat, U., Brandenburger, U., Dorn, H. P., Hausmann, M., Heßling, M., Holland, F., Plass-Dulmer, C., Sedlacek, M., Weber, M., and Ehhalt, D. H.: The measurement of tropospheric OH radicals by laser-induced fluorescence spectroscopy during the POPCORN field campaign and Intercomparison of tropospheric OH radical measurements by multiple folded long-path laser absorption and laser induced fluorescence – Reply, *Geophys. Res. Lett.*, 24, 3039–3040, 1997.
- Holland, F., Hessling, M., and Hofzumahaus, A.: In-Situ Measurement of Tropospheric OH Radicals by Laser-Induced Fluorescence – a Description of the KFA Instrument, *J. Atmos. Sci.*, 52, 3393–3401, 1995.
- Kukui, A., Ancellet, G., and Le Bras, G.: Chemical ionisation mass spectrometer for measurements of OH and Peroxy radical concentrations in moderately polluted atmospheres, *J. Atmos. Chem.*, 61, 133–154, doi:10.1007/s10874-009-9130-9, 2008.
- Malkin, T. L.: Detection of free-radicals and other species to investigate atmospheric chemistry in the HIRAC chamber, University of Leeds (School of Chemistry), 2010., Leeds, xvii, 285, 215 pp., 2010.
- Malkin, T. L., Goddard, A., Heard, D. E., and Seakins, P. W.: Measurements of OH and HO<sub>2</sub> yields from the gas phase ozonolysis of isoprene, *Atmos. Chem. Phys.*, 10, 1441–1459, doi:10.5194/acp-10-1441-2010, 2010.
- Mao, J., Ren, X., Zhang, L., Van Duin, D. M., Cohen, R. C., Park, J.-H., Goldstein, A. H., Paulot, F., Beaver, M. R., Crouse, J. D., Wennberg, P. O., DiGangi, J. P., Henry, S. B., Keutsch, F. N., Park, C., Schade, G. W., Wolfe, G. M., Thornton, J. A., and Brune, W. H.: Insights into hydroxyl measurements and atmospheric oxidation in a California forest, *Atmos. Chem. Phys.*, 12, 8009–8020, doi:10.5194/acp-12-8009-2012, 2012.
- Martinez, M., Harder, H., Kubistin, D., Rudolf, M., Bozem, H., Eerdeken, G., Fischer, H., Klüpfel, T., Gurk, C., Königstedt, R., Parchatka, U., Schiller, C. L., Stickler, A., Williams, J., and Lelieveld, J.: Hydroxyl radicals in the tropical troposphere over the Suriname rainforest: airborne measurements, *Atmos. Chem. Phys.*, 10, 3759–3773, doi:10.5194/acp-10-3759-2010, 2010.
- Novelli, A., Hens, K., Tatum Ernest, C., Kubistin, D., Regelin, E., Elste, T., Plass-Dulmer, C., Martinez, M., Lelieveld, J., and Harder, H.: Characterisation of an inlet pre-injector laser-induced fluorescence instrument for the measurement of atmospheric hydroxyl radicals, *Atmos. Meas. Tech.*, 7, 3413–3430, doi:10.5194/amt-7-3413-2014, 2014.
- Orkin, V. L., Martynova, L. E., and Ilchev, A. N.: High-Accuracy Measurements of OH Reaction Rate Constants and IR Absorption Spectra: CH<sub>2</sub>=CF-CF<sub>3</sub> and trans-CHF=CH-CF<sub>3</sub>, *J. Phys. Chem. A*, 114, 5967–5979, doi:10.1021/jp9092817, 2010.
- Park, J., Jongmsa, C. G., Zhang, R. Y., and North, S. W.: OH/OD initiated oxidation of isoprene in the presence of O<sub>2</sub> and NO, *J. Phys. Chem. A*, 108, 10688–10697, doi:10.1021/jp040421t, 2004.
- Pilling, M. J. and Seakins, P. W.: *Reaction Kinetics*, Oxford University Press, Oxford, 1995.
- Pilling, M. J., Bloss, W. J., and Wirtz, K.: IALSI: Processes relevant to global change – Improvements and Access to a Large Simulation Chamber, Fundacion CEAM, Valencia, Spain, 2005.
- Regelin, E., Harder, H., Martinez, M., Kubistin, D., Tatum Ernest, C., Bozem, H., Klippel, T., Hosaynali-Beygi, Z., Fischer, H., Sander, R., Jöckel, P., Königstedt, R., and Lelieveld, J.: HO<sub>x</sub> measurements in the summertime upper troposphere over Europe: a comparison of observations to a box model and a 3-D model, *Atmos. Chem. Phys.*, 13, 10703–10720, doi:10.5194/acp-13-10703-2013, 2013.
- Schlosser, E., Brauers, T., Dorn, H.-P., Fuchs, H., Hofzumahaus, A., Holland, F., and Wahner, A.: Intercomparison of Two Hydroxyl Radical Measurement Techniques at the Atmosphere Simulation Chamber SAPHIR, *J. Atmos. Chem.*, 56, 187–205, 2007.
- Schlosser, E., Brauers, T., Dorn, H.-P., Fuchs, H., Häsel, R., Hofzumahaus, A., Holland, F., Wahner, A., Kanaya, Y., Kajii, Y., Miyamoto, K., Nishida, S., Watanabe, K., Yoshino, A., Kubistin, D., Martinez, M., Rudolf, M., Harder, H., Berresheim, H., Elste, T., Plass-Dulmer, C., Stange, G., and Schurath, U.: Technical Note: Formal blind intercomparison of OH measurements: results from the international campaign HOxComp, *Atmos. Chem. Phys.*, 9, 7923–7948, doi:10.5194/acp-9-7923-2009, 2009.
- Schultz, M., Heitlinger, M., Mihelcic, D., and Volzthomas, A.: Calibration source for peroxy-radicals with built-in actinometry using H<sub>2</sub>O and O<sub>2</sub> photolysis at 185 nm, *J. Geophys. Res.-Atmos.*, 100, 18811–18816, doi:10.1029/95jd01642, 1995.
- Singh, S. and Li, Z. J.: Kinetics investigation of OH reaction with isoprene at 240–340 K and 1–3 Torr using the relative rate/discharge flow/mass spectrometry technique, *J. Phys. Chem. A*, 111, 11843–11851, doi:10.1021/jp074148h, 2007.
- Sjostedt, S. J., Huey, L. G., Tanner, D. J., Peischl, J., Chen, G., Dibb, J. E., Lefer, B., Hutterli, M. A., Beyersdorf, A. J., Blake, N. J., Blake, D. R., Sueper, D., Ryerson, T., Burkhardt, J., and Stohl, A.: Observations of hydroxyl and the sum of peroxy radicals at

- Summit, Greenland during summer 2003, *Atmos. Environ.*, 41, 5122–5137, 2007.
- Stevens, P. S., Mather, J. H., and Brune, W. H.: Measurement of Tropospheric OH and HO<sub>2</sub> by Laser-Induced Fluorescence at Low-Pressure, *J. Geophys. Res.-Atmos.*, 99, 3543–3557, 1994.
- Stone, D. and Rowley, D. M.: Kinetics of the gas phase HO<sub>2</sub> self-reaction: Effects of temperature, pressure, water and methanol vapours, *Phys. Chem. Chem. Phys.*, 7, 2156–2163, 2005.
- Wennberg, P. O., Cohen, R. C., Hazen, N. L., Lapson, L. B., Allen, N. T., Hanisco, T. F., Oliver, J. F., Lanham, N. W., Demusz, J. N., and Anderson, J. G.: Aircraft-Borne, Laser-Induced Fluorescence Instrument for the in-Situ Detection of Hydroxyl and Hydroperoxyl Radicals, *Rev. Sci. Instrum.*, 65, 1858–1876, 1994.
- Whalley, L. K., Furneaux, K. L., Gravestock, T. J., Atkinson, H. M., Bale, C. S. E., Ingham, T., Bloss, W. J., and Heard, D. E.: Detection of iodine monoxide radicals in the marine boundary layer using laser induced fluorescence spectroscopy, *J. Atmos. Chem.*, 58, 19–39, 2007.
- Whalley, L. K., Furneaux, K. L., Goddard, A., Lee, J. D., Mahajan, A., Oetjen, H., Read, K. A., Kaaden, N., Carpenter, L. J., Lewis, A. C., Plane, J. M. C., Saltzman, E. S., Wiedensohler, A., and Heard, D. E.: The chemistry of OH and HO<sub>2</sub> radicals in the boundary layer over the tropical Atlantic Ocean, *Atmos. Chem. Phys.*, 10, 1555–1576, doi:10.5194/acp-10-1555-2010, 2010.
- Whalley, L. K., Blitz, M. A., Desservettaz, M., Seakins, P. W., and Heard, D. E.: Reporting the sensitivity of laser-induced fluorescence instruments used for HO<sub>2</sub> detection to an interference from RO<sub>2</sub> radicals and introducing a novel approach that enables HO<sub>2</sub> and certain RO<sub>2</sub> types to be selectively measured, *Atmos. Meas. Tech.*, 6, 3425–3440, doi:10.5194/amt-6-3425-2013, 2013.
- Winiberg, F. A. F.: Characterisation of FAGE apparatus for HOx detection and application in an environmental chamber, Ph.D, School of Chemistry, University of Leeds, Leeds, 233 pp., 2014.